The R-Process, 1957 to 2002

A. G. W. Cameron

Invited talk at the Michigan R-Process Workshop

This web posting contains the viewgraphs and figures of my talk at the workshop, with additional commentary designed to make them a little less mysterious.

I start with a brief history of stellar nucleosynthesis before concentrating on the r-process and related topics (see Viewgraph 1). It seems appropriate to start with the concept of Coulomb barrier penetration. This is usually attributed to Gamow (1929), but in fact there was a paper by Gurney and Condon (1929)) on the same subject. In the late 1930s Bethe (1939) and von Weizsäcker (1937 and 1938) worked out some of the details of hydrogen burning in an attempt to understand the long-lived maintenance of stellar luminosities, which had much earlier been attributed to gravitational contraction as the energy source.

Interestingly enough, the last step in stellar evolution was investigated at about the same time. Oppenheimer and Volkoff (1939) made the first calculations of the structure of neutron stars (with no attempt to include nuclear forces), and Oppenheimer and Snyder (1939) considered the contraction of a stellar mass greater than the neutron star upper limit, and found that it had to be in a state of continued contraction (they did not call it a black hole). Also, slightly earlier, Baade and Zwicky (1934) studied supernovas, and suggested that they developed neutron cores. So the concept of massive spheres of neutrons had an early start.

Shortly after World War II Fred Hoyle (1946) published his calculations relating to the formation of the elements, assuming that the elements resulted from nuclear statistical equilibrium under various conditions. Also after the war Willy Fowler and his colleagues at the Kellogg Radiation Laboratory at Caltech began measuring the thermonuclear reaction rates of the basic hydrogen-burning reactions in the Sun and stars using their low energy particle accelerator.

Several key developments occurred during the 1950s. Edwin Salpeter (1952) developed the theory of the triple-alpha reaction of helium-burning, and Martin Schwarzschild started calculating stellar models and their evolution through these stages. Paul Merrill (1952) discovered the lines of technetium in red giant

stars of class S. I identified the $^{13}C(\alpha,n)^{16}O$ reaction as having produced them (Cameron 1955) and started doing calculations of s-process nuclear reaction networks. Walter Baade (1957) was able to classify stars into older Population II stars and younger Population I stars; the older ones generally had weaker lines of the heavier elements and thus established the basis for galactic chemical evolution, indicating that stars in general must be element-generating engines that progressively enrich the galaxy in their products.

But equally important was the development of cosmochemistry. Hans Suess had for some time been trying to determine the cosmic abundances of the elements, using empirical means to interpolate the elements and their nuclides where the abundances had not been measured (and what measurements there were were often very crude and of uncertain generality). Then he combined with Harold Urey and in 1956 they published their classic paper on abundances. What a boon to nuclear physicists! Willy Fowler and his colleagues started identifying stellar mechanisms that could produce these abundances, and so did I. The nomenclature that we use today is derived from Fowler's classification, which differs slightly from the one I developed.

The r-process was one of these processes (I called it neutron capture on a fast time scale). B^2FH (Burbidge, Burbidge, Fowler and Hoyle (1957)), in looking at the r-process, put forward the ^{254}Cf theory of Type I supernova light curves, according to which this isotope, with a half life of 55 nights, became the principal energy source for the light curve because it decayed predominantly by spontaneous fission (see Figure 1). These studies led to the important concept of the r-process waiting points. I think this concept was due to Fred Hoyle, because a waiting point is a local area of statistical equilibrium between neutron capture and loss, which is the kind of thinking that he liked to do. See Figures 2 and 3.

Meanwhile I was systematically studying the successive stages of stellar nuclear burning, approaching the end point at which the star would settle down as a white dwarf or collapse to a supernova. I returned to the problem of the totally collapsed configuration, added some crude nuclear forces to the equation of state for a neutron star, and considered the composition as modified by the inclusion of hyperons and muons to the mixture.

At the end of the 1950s John Reynolds diversified the field in yet another important way, by discovering traces of the decay of the extinct nuclide ^{129}I in meteoritic material, thus opening up the diverse field of cosmochronology.

Early Developments in Stellar Nucleosynthesis

- **Gamow: Coulomb Barrier Penetration**
- **Bethe, von Weissacker: Hydrogen Burning**
- **Oppenheimer: Neutron Stars, Black Holes**
- **Baade, Zwicky: Supernovas, Neutron Cores**
- **Hoyle: Equilibrium Theory of Element Formation**
- **Fowler: Cross Section Measurements**
- **Öpik, Hoyle, Salpeter: Triple Alpha Reaction**
- **Schwarzchild: Stellar Models and Evolution**
- **Merrill: Technetium Lines in S Giants**
- **Cameron: ^{13}C(α,n)^{16}O Neutron Source**
- **Baade: Galactic Evolution: Element Synthesis**
- **Suess and Urey: Table of Element Abundances**
- **B^{2}FH, Cameron: Nucleosynthesis Processes Classification**
- **Cameron: Studies of the S-Process, Stellar Burning Stages**
- **B^{2}FH: ^{254}Cf Theory, R-Process Waiting Points**
- **Cameron: Neutron Star Composition, Structure**
- **Reynolds: ^{129}I, First Extinct Radionuclide in Solar System**

Viewgraph 1

The early approach to the r-process generally assumed that because of the short time scales involved, the process must be associated with supernova explosions in some way. See Viewgraph 2. It was clear that large fluxes of neutrons would be required, but it was not clear how these were to be generated. So the initial investigations simply assumed a high neutron number density and concentrated on solving the nuclear physics problems of how the neutron capture flows would go in the presence of the high neutron flux. One adjusted the

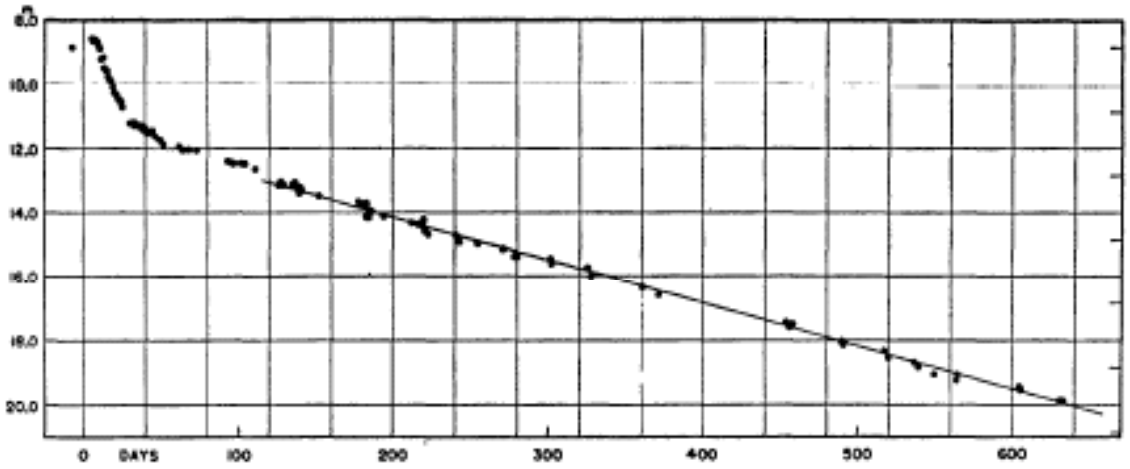

FIG. 1.—Photographic light curve of the supernova in IC 4182. The abscissa gives the time after maximum, in days; the ordinate gives the apparent photographic magnitude.

Figure 1. Walter Baade's supernova light curve with the 55 night half-life.

neutron number density and the temperature in such a way as to reproduce the abundance distibution of the r-process isotopes, assuming that one had successfully calculated the masses and beta decay half lives of the nuclei well on the neutron-rich side of the valley of beta stability. It was clear that the r-process abundance humps were associated with the closed neutron shells in nuclei. A question that I do not think was ever asked was whether such calculations would stand up if the r-process took place in the presence of a high electron degenerate Fermi level, which would exclude many of the assumed beta decay branches at the waiting points and hence lengthen the beta decay half lives.

Going beyond these early insights required identifying the source of the neutrons. The early hopes of getting them through thermonuclear production (such as for the s-process) were unfulfilled when simulations proved inadequate. So investigations moved toward utilization of the large reservoir of neutrons created when a core collapse supernova created a neutron star remnant through compression and electron capture on the constituent nuclei near the center of the presupernova. Of course, then the question became, how can these neutrons be utilized? Since a neutron star is in principle a static configuration (at least after it has radiated most of its energy in neutrinos and antineutrinos), then one must arrange to extract the neutrons from the neutron star. At first such an

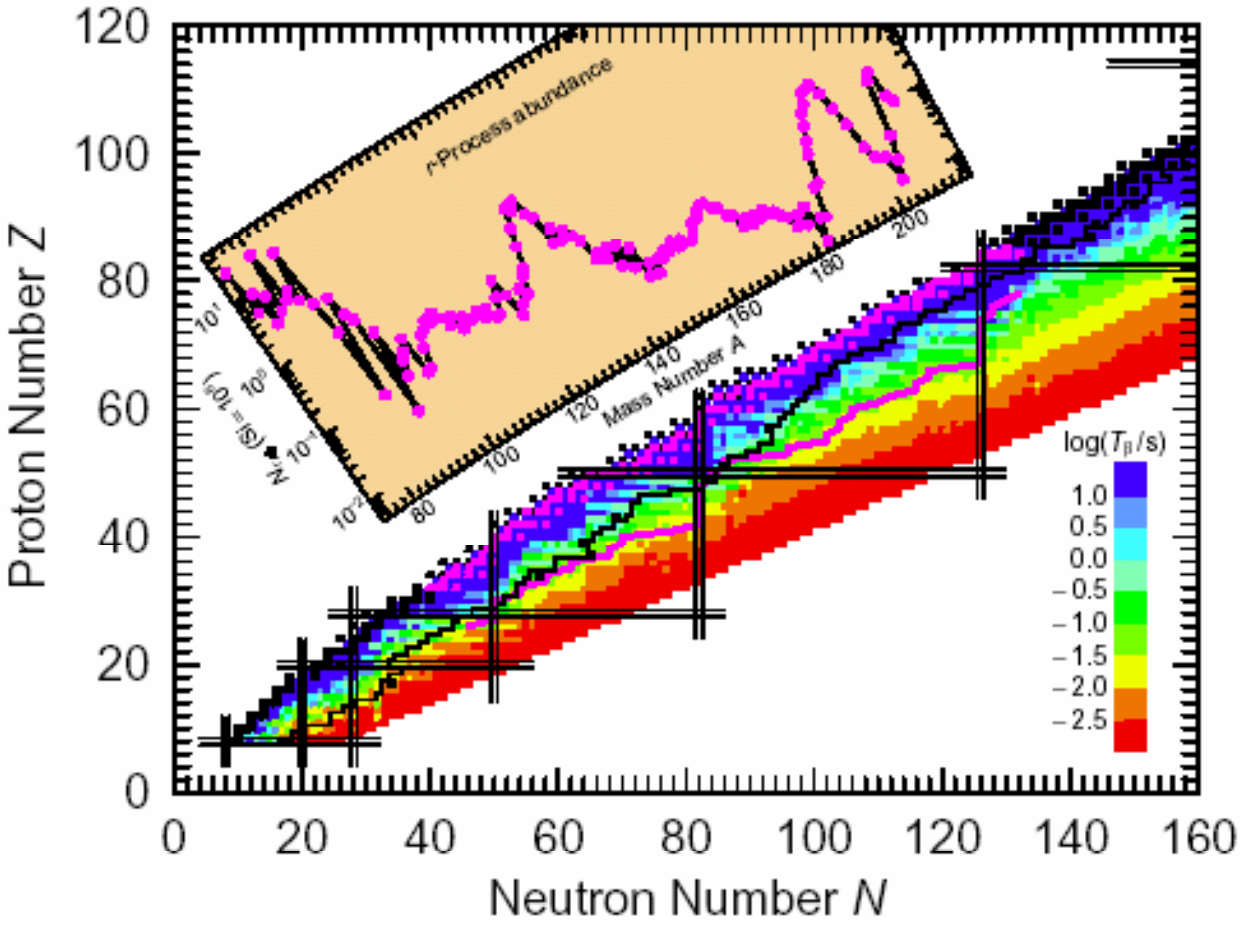

Figure 2: A chart of the nuclides (after *10*). At a given proton (atomic) number, isotopes toward the left are proton-rich and those to the right are th neutron-rich ones that are the subject of this paper. The stable nuclides are marked by black boxes and n-capture in s-process synthesis occurs near these nuclei close to the "valley of beta stability." The jagged diagonal black line represents the limit of experimentally determined properties of nuclei and the magenta line the r-process "path." Vertical and horizontal black lines represent closed neutron or proton shells, sometimes referred to as "magic numbers." Color shading denotes the different (log) timsecales for beta-decay.

Figure 2. A nuclide chart showing details of the r-process. Courtesy of C. Sneden and J. Cowan.

extraction process seemed most likely to be associated with dynamical events intrinsic to the supernova explosion itself. This gave rise to investigations of the neutron blow-off from the surface of the nascent neutron star as a result of the large flux of neutrinos and antineutrinos emerging from the interior. See Viewgraph 3.

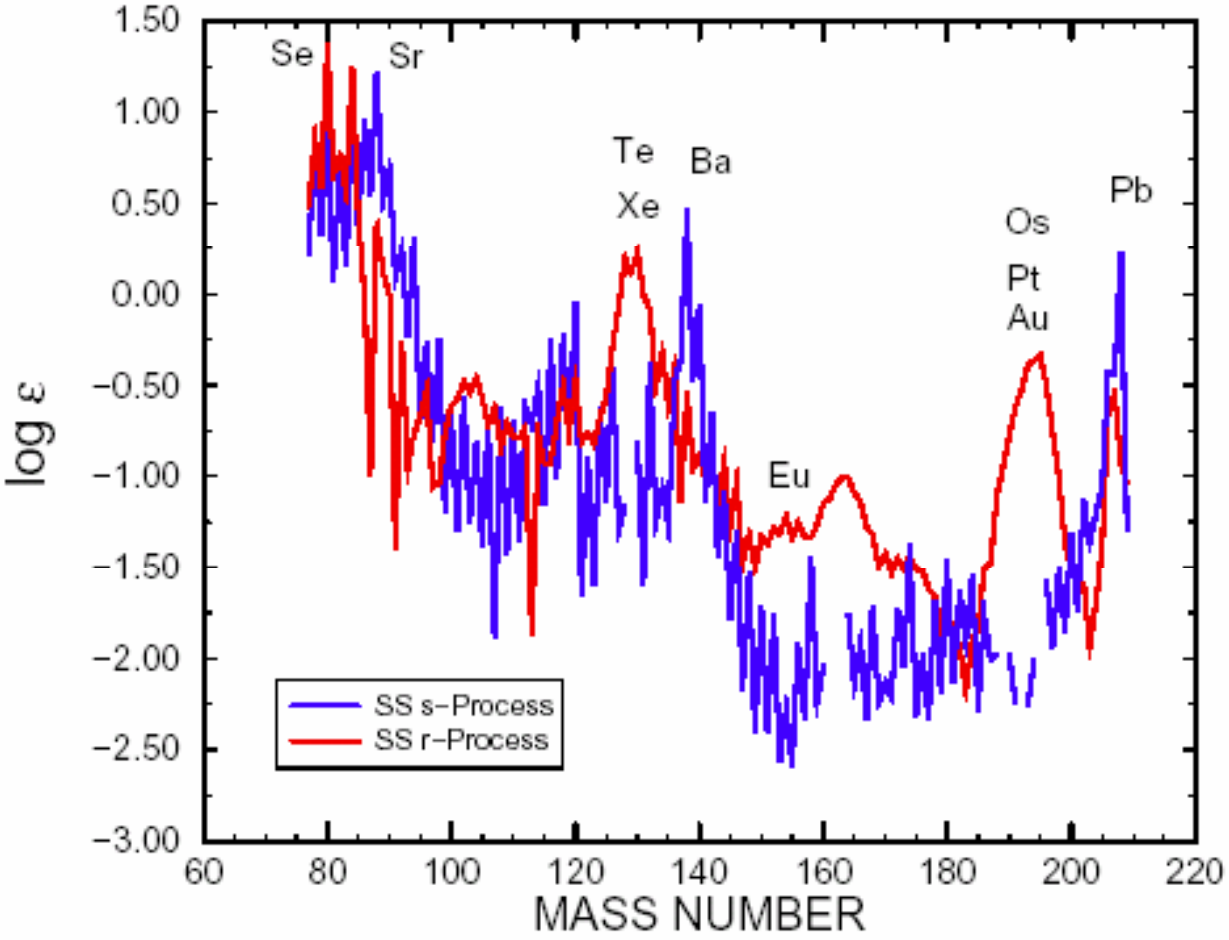

Figure 4: The breakdown of solar system (meteoritic) n-capture isotopic abundances into r- and s-process components (based upon 5). The approximate mass numbers corresponding to some prominent elements are noted.

Figure 3. The abundance distributions for the s- and r-processes. Some elements of importance in studies of ultra-metal-poor stars are shown. Courtesy of C. Sneden and J. Cowan.

The investigations of Qian and Woosley (1996) of this scenario initially seemed very promising, and a lot of useful insight into the conditions at the neutron star surface were obtained. But the further investigations with Hoffman (*et al.* 1997) showed that an r-process build-up could only go about as far as the 50 neutron closed shell, and that the entropy in the wind would have to be raised to an unattainably high level in order to go the rest of the way to a full r-process. So progress in understanding the r-process stagnated.

Early Thoughts About the R-Process

• AGWC: How can we minimize the neutron to seed ratio? Tentative approach: First build up to heavy elements by the s-process. Then irradiate this with a sudden flood of neutrons. They would have to come from explosive burning of ^{13}C(α,n)^{16}O. This counts on higher cross sections in heavy nuclei to preferentially capture neutrons relative to light abundant nuclei. But this does not work out. Reason: When a heavy nucleus advances to a waiting point, it sits there while the neutrons are then captured on light nuclei.

• B^{2}FH: The ^{254}Cf hypothesis requires that there be an even bigger flood of neutrons than postulated above. This allows development of the association of r-process abundance peaks with neutron closed shells, analogous to the s-process, with corresponding r-process waiting points. But the source of the neutrons remained a major mystery. Since a waiting point is an equilibrium process, this concept was probably developed by Fred Hoyle, who primarily thought in those terms.

• Everyone: This led to many years in which people working on the r-process simply assumed that there would be a suitable source of neutrons somewhere in supernova explosions. They concentrated on improving the nuclear physics of the nuclei out near the neutron drip lines and simulating irradiations with high neutron fluxes trying to achieve good fits to the r-process peaks.

• In the last two decades: People have realized: If you want lots of neutrons, go where you know there are lots of neutrons. Neutron stars and protoneutron stars.

Viewgraph 2

But there are other ways to get matter out of a neutron star, if it encounters another massive and dense body. If a neutron star comes close to a black hole, then surface material may be ejected by tidal stripping. Or if two neutron stars

Neutron Star Winds

• Theoretical studies of Core-Collapse Supernovas gradually revealed that the explosive mechanism depended critically on the intense flood of neutrinos and antineutrinos (all three flavors) travelling through the collapsed structure and depositing energy and momentum. After an outgoing shock has driven off the envelope, the outer layers of the neutron star remnant are hot enough (10^{10} degrees) to cause the hydrodynamic expulsion of a neutron wind, which also contains protons and alpha-particles.

• Woosley and Hoffman (1992) tried to follow the build-up of seed nuclei in this wind and the subsequent r-process that would develop out of it. The formation of seed nuclei is sensitive to the conditions in which the ^{4}He(αn,γ)^{9}Be(α,n)^{12}C reaction competes with the triple-alpha reaction. Woosley and Hoffman found that they needed to have this wind at extremely high entropy, which Woosley has never been able to justify from the detailed physics of the process.

• Hoffman, Woosley, and Qian (1997) studied the r-process in the expanding wind under conditions that they could justify (much lower entropy). They found that the r-process could build up nuclei to about A = 80 (at the N = 50 closed shell), but they could not get the heavy end of the r-process. It became clear that either major modifications would be needed in their model or an entirely different model would be required.

Viewgraph 3

collide, then the kinetic energy of the collision would be sufficient to eject material, particularly if the collision was a glancing one, such as would occur if the two neutron stars were part of a binary system. Freiburghaus *et al.* (1999) studied this scenario and found that they could get an r-process.

However, such an event is extremely rare. It fails to account for the r-process extinct radioactivities in the solar system (see below) for timing reasons. The

time required for the products to diffuse through the galaxy to significant fractions of the distances between such events is very long compared to the half lives of these extinct radioactivities. Also, the r-process is a significant feature of the earliest generations of stars (see below). But the time for binary neutron star pairs to come together through orbital decay by gravitational radiation is generally too long to have produced the heavy elements by this r-process in the earliest stellar generations. Thus this process fails two timing constraints to be identified as the general source of the r-process products, although it might eventually produce them in a few localized regions.

However, in 2000 I started pondering why the neutron star wind model for the r-process had not worked. It was based on excellent treatments of the nuclear physics and energy transport mechanisms. Could it be that the astrophysical model was too simple? Astrophysicists usually omit complications such as magnetic fields and rotation. A core-collapsing supernova would surely have angular momentum and magnetic fields in the interior. When the collapse takes place, the interior density gradient in the presupernova would require the central region to collapse faster than the outer layers, so that conservation of angular momentum would cause differential rotation to occur. This would wrap the magnetic field lines into a toroid, and its expansion would increase the pressure in the equatorial plane, adding an additional flattening to that which would already be associated with the rotation (see Figure 4). The disk formed in this way can be called an extrusion disk. Since rotation would also form a disk, and dissipation would make this an accretion disk, the combined effects can be described as an accretion-extrusion disk (Cameron 2001).What would be its properties?

Mario Livio (1999) has pointed out that all known astrophysical objects with accretion disks have associated bipolar jets (see Viewgraph 4). It is thus a reasonable assumption that this protoneutron star would also acquire jets. The principal function of a jet is to remove angular momentum from a star (or from a major component of a galaxy). In this case it would extract angular momentum from both the accretion and the extrusion flows where they would meet near the equator of the star. Studies of relativistic jets have predicted that the outflow velocity in a jet should be about equal to the Keplerian velocity in the disk at the roots of the jet. In this case that means that the outflow velocity would be about $0.5c$, where c is the velocity of light. This corresponds to particle energies of 140 MeV per nucleon.

R-Process Accretion-Extrusion Disks and Jets

- **Why did the Woosley-Qian model of the neutron star wind fail to provide a full r-process? How could it be modified? What was omitted? Answer: rotation and magnetic fields.**
- **Rotation: When a rotating presupernova collapses to form a neutron star, conservation of angular momentum will form a disk around it in the equatorial plane. This disk will be subject to dissipation and hence to accretion.**
- **The magnetic field embedded in the presupernova will be wrapped into a toroid during the collapse because the center collapses faster and therefore rotates faster than the descending envelope. The strengthening toroidal field will push matter out in the equatorial plane, so that matter becomes an extrusion disk.**
- **Livio has pointed out that every astronomical object with a magnetized accretion disk forms a pair of jets to help conserve angular momentum. Livio's list of such objects is as follows: active galactic nuclei, young stellar objects, massive x-ray binaries, low mass x-ray binaries, black hole x-ray transients, symbiotic systems, planetary nebulae, and supersoft x-ray sources. We must therefore expect that neutron star magnetized accretion-extrusion disks will also form a pair of jets.**
- **The magnetic field in the jets will be spirally wound with roots in the disk near the neutron star equator. A neutron star wind may still be emitted above a latitude of about 60 degrees from the equatorial plane, within the cone formed by the jets. The ejection velocity will be about equal to the Keplerian velocity of material in the roots. In this case that means the jet velocity is $\sim 0.5c$, or about 140 MeV per nucleon.**

Viewgraph 4

There would be no sharp boundary between the disk and the neutron star; one would smoothly merge into the other. In the accretion disk the initial tem-

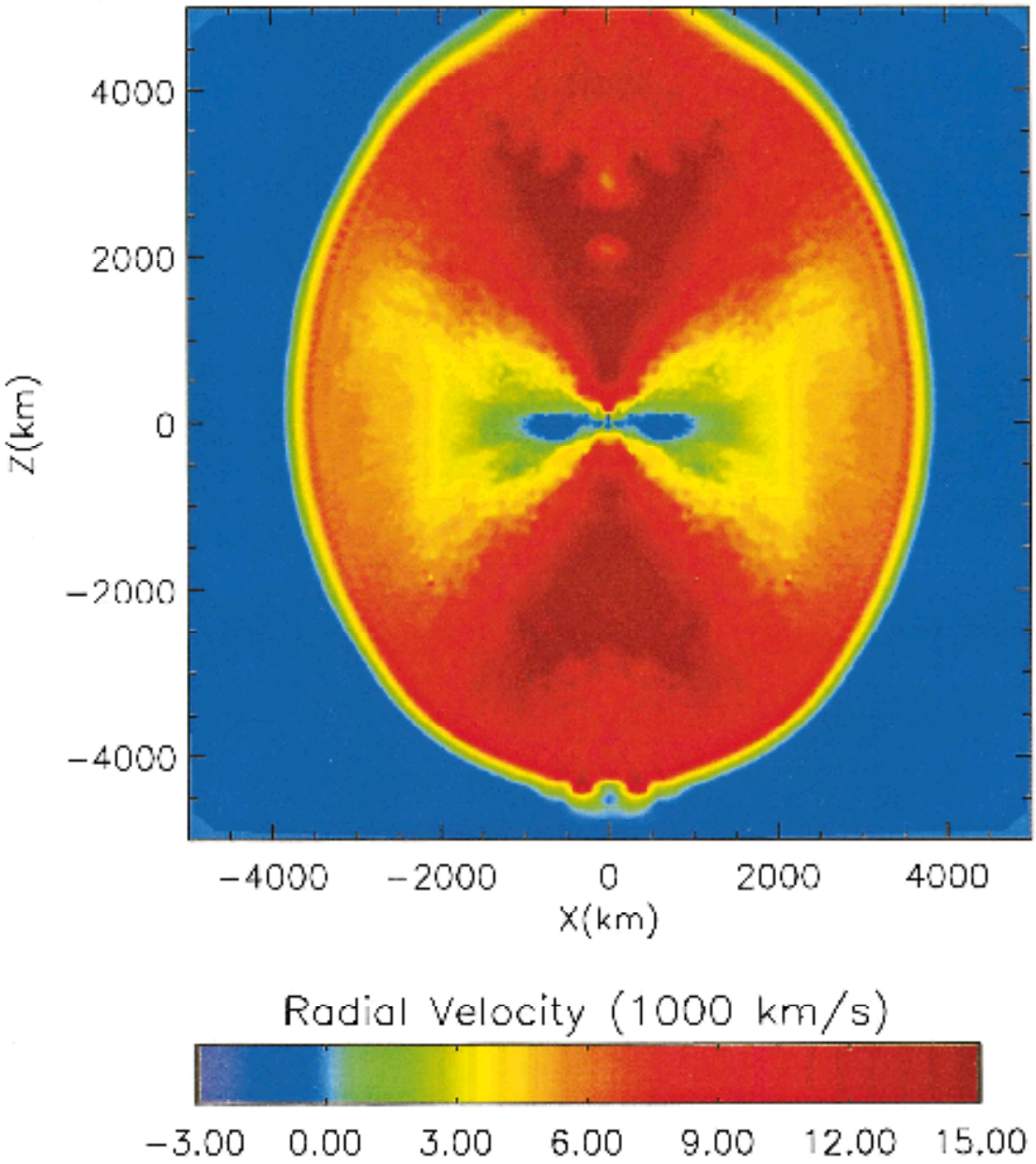

Figure 4. A simulation of a core collapse supernova with rotation added. C. L. Fryer and A. Heger, *Astrophys. J.*, **541**, 1033 (2000).

perature would be about 10^{10} K, as in the Qian and Woosley discussion. So the nuclei would be in nuclear statistical equilibrium throughout the entire configuration. In the outer disk the nuclei would thus form a peak in the viciniy of mass numbers 90 to 100 (see Viewgraph 5). Farther in towards the neutron star, nuclear statistical equilibrium will maintain roughly the same abundance shape as the neutron drip line is approached at higher densities. Beyond the drip line an increasingly large number density of free neutrons will be maintained. At

Jet Contents and the R-Process

- **Because of the accretion-extrusion nature of the disk, matter should enter the jets from densities both smaller and larger than that at the jet roots (taken to be at about 10^{11} gm/cm^3. Temperature probably initially about 10^{10} degrees and cooling.**

- **Lower density: Matter in neutron-rich nuclear statistical equilibrium. The abundance peak should lie in the range A = 90 to 100.**

- **Higher density: Nuclear statistical equilibrium abundance peak still around A = 90 to 100, but beyond the ordinary neutron drip line, so nuclei are in equilibrium with a sea of free neutrons just like the situation in an ordinary neutron star outer envelope. The ratio of free neutrons to seed nuclei rises rapidly with increasing density. In equilibrium, the r-process cannot operate, so the material cools due to energy loss in a general URCA process in which rates of neutrino and antineutrino emission are equal.**

- **When the jets operate, matter will be fed into the roots from both lower and higher density regions. This starts the r-process slowly, because in material moving toward lower density, the electron Fermi level is reduced, and phase space is opened for increased beta decay rates while electron capture rates are decreased. A conventional r-process freeze-out should occur with familiar r-process abundance patterns as the material moves into the jets. For the material coming from lower density regions, the main effect is beta decay with some delayed neutron emissions.**

Viewgraph 5

---

the valley of beta stability, within the nuclear potential well the neutrons and protons fill the levels up to about the same energy. At increasingly higher densities the neutrons fill the levels in the well to higher energies, and the protons

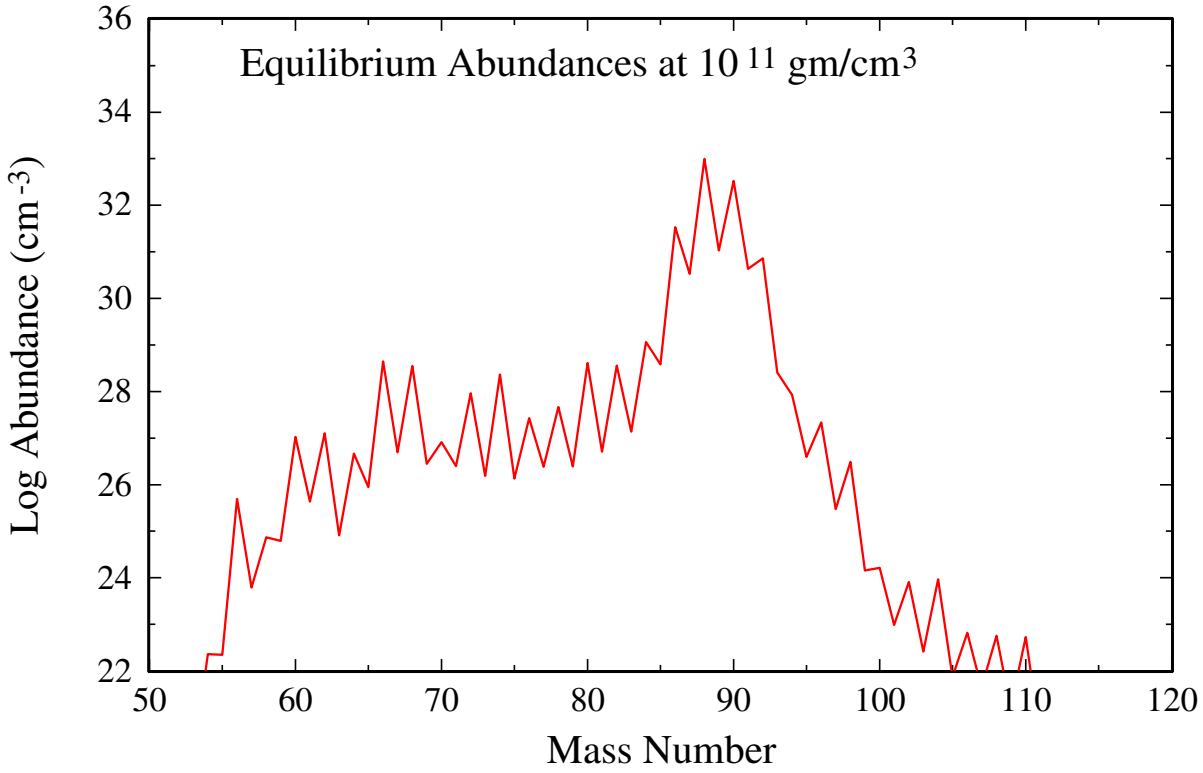

Figure 5. Nuclear statistical equilibrium abundances in the outer accretion disk.

only fill the levels to lower energies. The energy difference between them is roughly equal to the electron Fermi energy. Beyond the drip line the neutrons not only fill the well but form a degenerate neutron gas extending to a neutron Fermi level above the top of the well (and they are not confined to the vicinity of the well).

The seed nuclei for the r-process consist of the abundance distribution for nuclear statistical equilibrium in the outer layers of the neutron star. This is probably similar to that shown for smaller densities in Figure 5, although the effects on the abundances due to the neutron shell effects near the neutron drip line and of the presence of the degenerate Fermi sea of neutrons have been insufficiently examined. Starting near mass number 90, the r-process build-up toward heavier nuclei should go to at least mass number 300 before fission occurs. In general terms without regard to particular nuclear structure effects, the fission probability increases with the ratio Z^2/A, which is proportional to

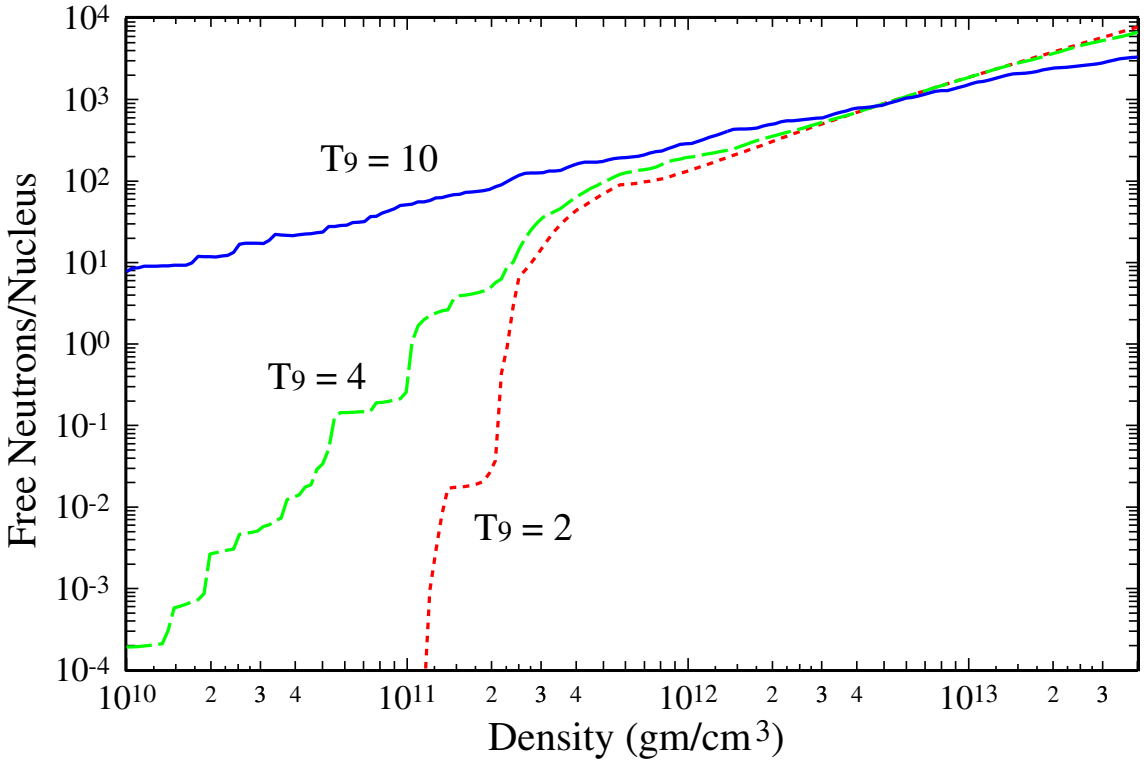

Figure 6. Free neutron number densities going in to the neutron star.

the ratio of the volume electrotatic energy to the surface energy of the nucleus. This means that for any given element, the fission probability decreases for increasing mass number. Thus the fission point along the r-process capture path should be higher in mass number earlier when the capture path is beyond the neutron drip lines than it will be later when the capture path is about at a neutron binding energy of 2 MeV which is characteristic of the r-process freeze-out. Thus for an r-process that extends up to the fission point and produces two nuclei at lower mass number, the seed nuclei need to capture about 150 or more neutrons each before fissioning. From Figure 6 we can thus see that the r-process starting point needs to be at about a density of 10^{12} gm/cm^3 or higher. Figures 7 and 8 show how I have extrapolated fission properties to estimate where the r-process fission recycling would occur, at least in the late stages when the r-process capture path has moved to the left of the neutron drip lines to about the nucleus ^{297}Bh. Figure 9 shows where the fission peaks from this

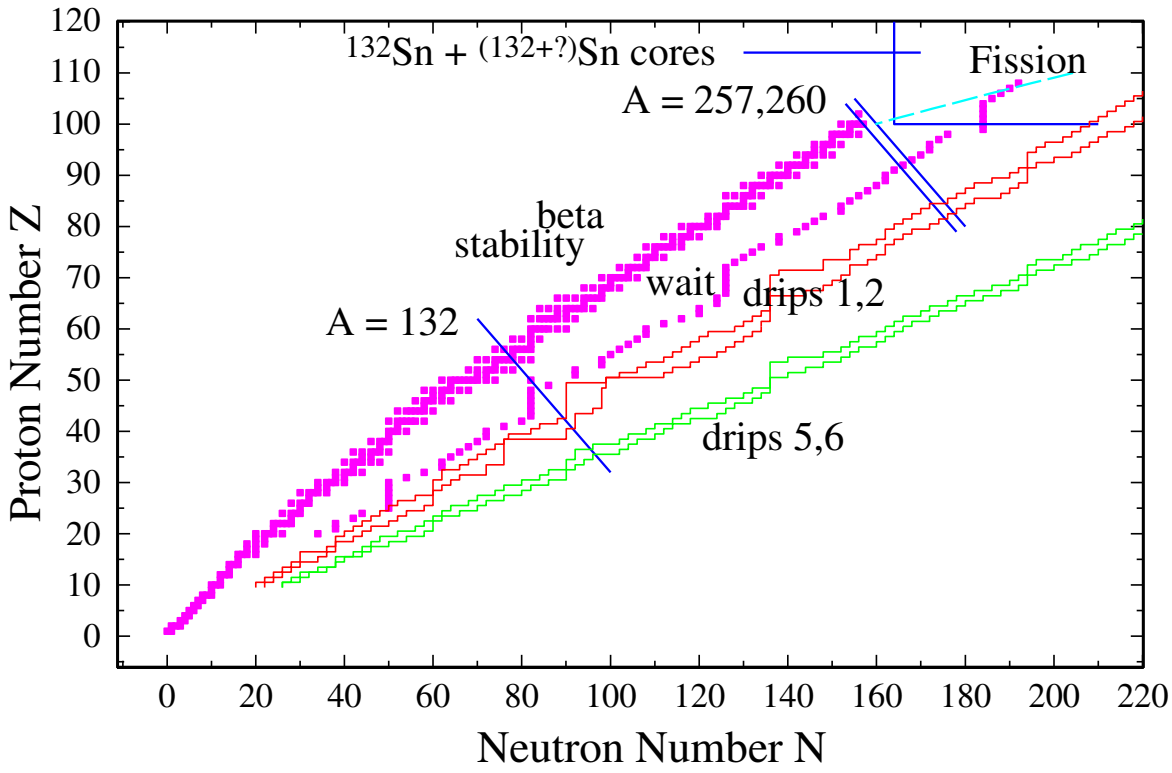

Figure 7. A nuclide chart showing the stable nuclei along the valley of beta stability as solid squares and also an approximate set of neutron capture waiting points marked "wait" where the neutron binding energy falls below 2 MeV. The box in the upper right corner shows where fission fragments will primarily each have a ^{132}Sn doubly closed shell core inside. The line marked A = 257 shows where r-process beta decay starts leading to fissioning nuclei, and the line marked A = 132 shows where at least one of the fission fragments should approximately be formed. The lines marked "drips 1,2" show the location of the actual drip lines at low densities. Drip 1 is where every second nucleus at a given Z becomes neutron unstable, and drip 2 is where all nuclei for that Z become unstable. "Drips 5,6" shows the effective drip lines for these two conditions at a density of 10^{13} gm cm^{-3} due to the presence of a neutron Fermi energy of 6.4 MeV.

---

fission point are likely to lie, and that the higher one coincides with a prominent r-process hump in the rare earth region at about A = 165. See Cameron (2003)

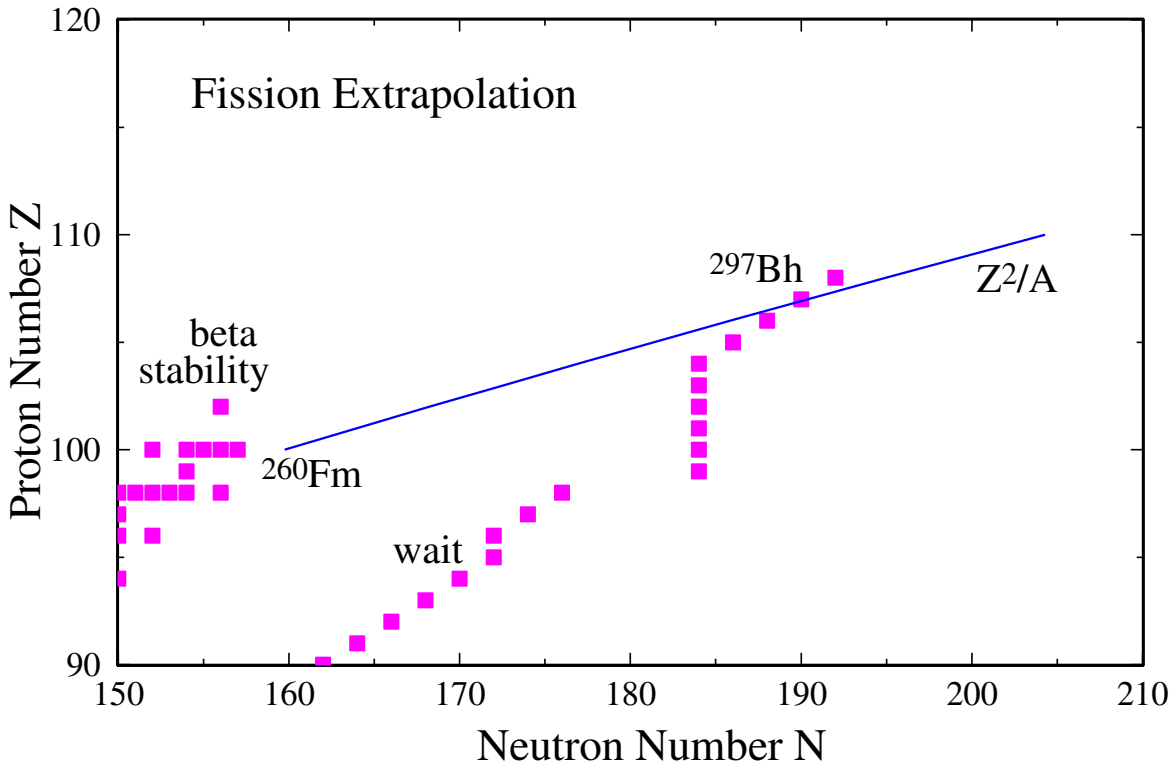

Figure 8. This is an enlargement of the upper right corner of Figure 7, although the box lines have been omitted. The solid rectangles on the left are the upper end of the valley of beta stability, while those in the middle of the graph mark the positions of the last nucleus for each Z at which the neutron binding energy is above 2 MeV (the late stage waiting points of the r-process). The line marked 'Z^2/A' is the fissility extrapolation from ^{260}Fm, intersecting the neutron capture path at ^{297}Bh.

for more details. Figure 10 shows an extract from a 1957 nucleosynthesis review by me that guessed at this outcome.

Meanwhile, the inward accretion flow from the outer part of the accretion-extrusion disk will also be feeding material into the roots of the jets, but without mixing the two streams of material, which form alternating spiral wrappings in the jets. The convergence of the accretion and extrusion streams of material into the roots of the jets should keep the roots constrained within a rather narrow radial interval, and thus the jets themselves should have thin walls. The opening

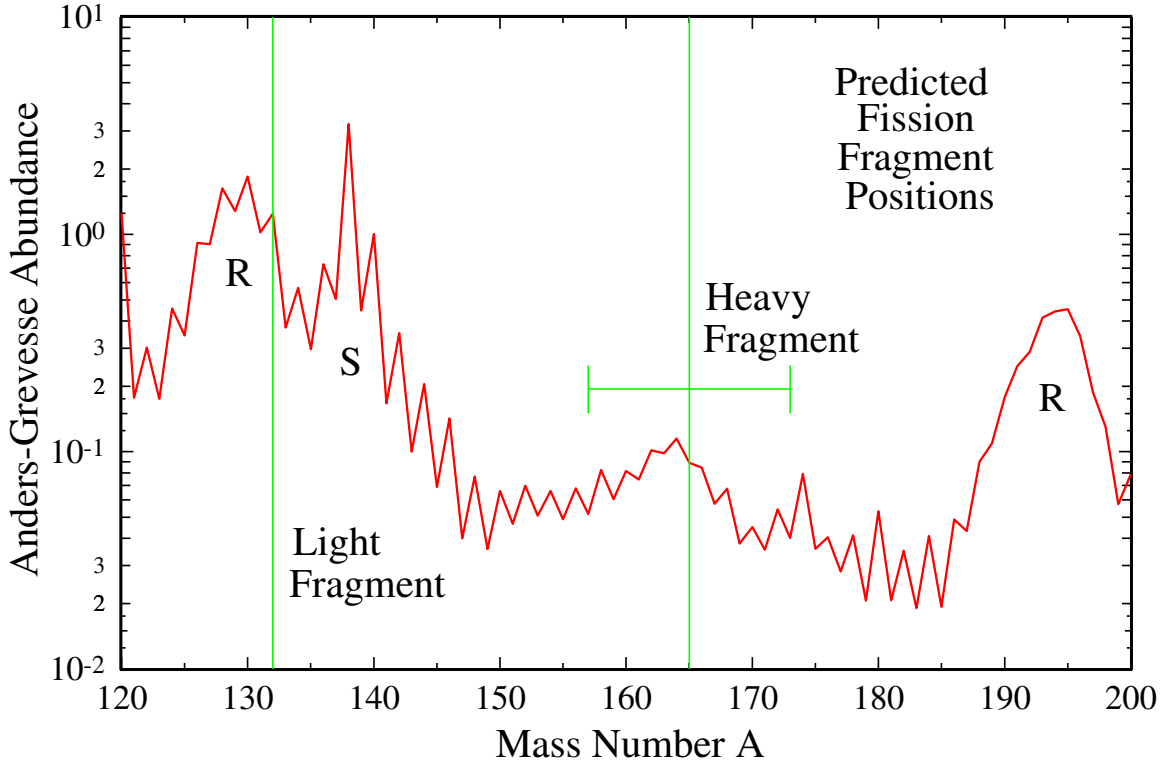

Figure 9. The approximately predicted fission fragment peak positions that would be produced by the fission of ^{297}Bh, compared with the nuclide abundance distribution of Anders and Grevesse.

angle of the jets must remain small since there will be a hoop stress exerted on the jets. Bipolar outflow theory applied to a thin disk predicts that matter will be elevated along the spiral wrappings as long as the angle at which the magnetic lines of force emerge from the disk does not exceed 60 degrees above the equatorial plane (Königl and Pudritz 2000). Once the material is elevated the hoop stress (z-pinch) will bend the jet toward the vertical.

Under static conditions the r-process cannot occur inside the neutron star itself. The material there reaches nuclear statistical equilibrium subject to the constraint that the rates of emission of neutrinos and antineutrinos must become equal (this is called the URCA process). Such emission rapidly cools the neutron star in the absence of additional heating processes. However, when material undergoes extrusion, the r-process can commence, slowly at first. As material

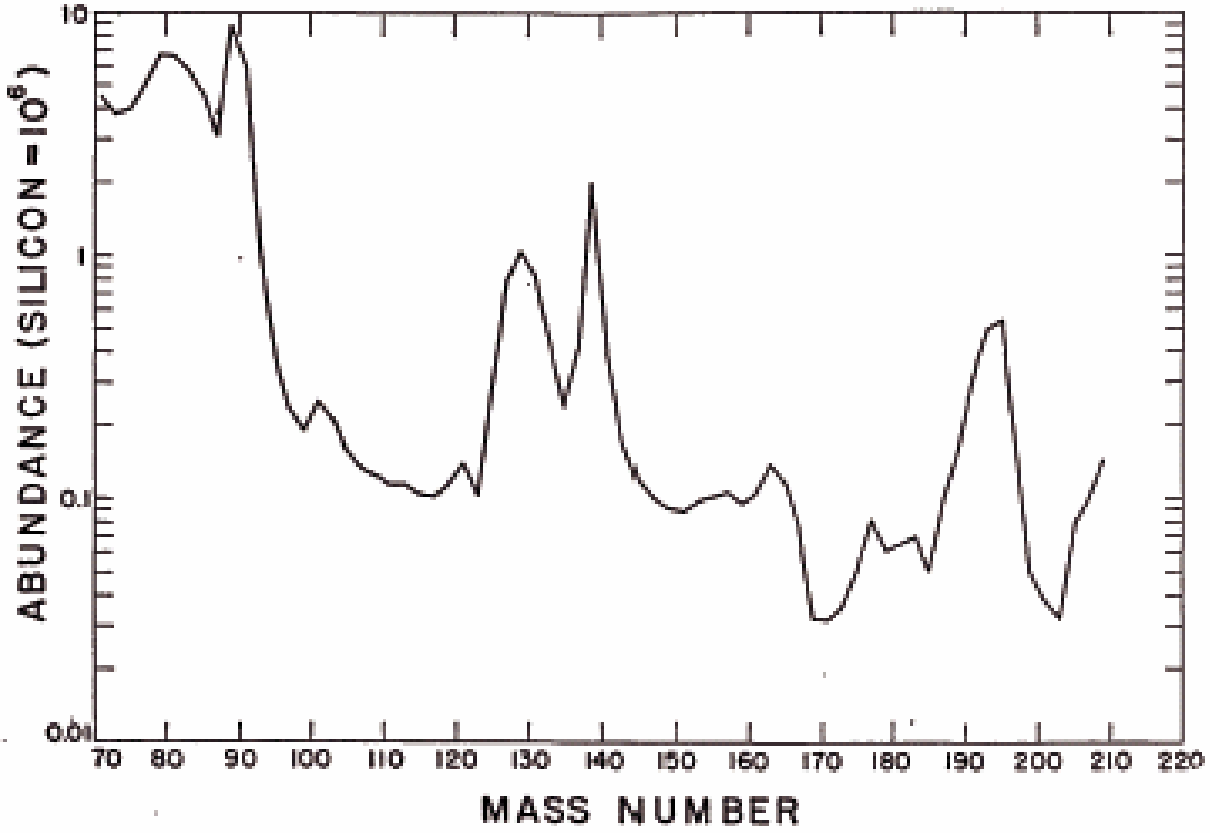

FIG. 7.—The cosmic abundances of nuclides with odd mass number according to Suess and Urey.

tron capture on a slow time scale such as is expected to occur during the early stages of helium consumption in a star. The subsidiary peak at mass number 160 may be formed by the spontaneous fission of very heavy nuclei formed by neutron capture on a fast time scale.

Figure 10. Extract from PASP, **69**, 201 (1957)

moves toward lower density, the electron Fermi energy is reduced. Then (1), phase space is opened up for beta decays to take place, and (2), the rate of electron capture is reduced. So now there are beta decay waiting points, but initially they lie much farther to the neutron-rich side of the valley of beta stability, in fact beyond the neutron drip lines. The rate of the r-process accelerates as

the material approaches the base of the jets, and it should exhaust most of the available free neutrons when it is in that vicinity. As the material is accelerated upwards in the jets, the beta decay toward the valley of beta stability will take place, and the conventional calculations of this phase should be applicable to it. The r-process component of the material will then become a strong gamma-ray emitter as the beta decay occurs.

The surface of the neutron star at higher latitudes is likely to emit a neutron wind as long as there is a strong flux of neutrinos and antineutrinos emerging from the center of the nascent neutron star, in the manner predicted by Qian and Woosley (1996). However, their work was based on the assumption that the emitting surface was at relatively low density and high temperature (10^{10} K), so that the surface material was broken down into just neutrons mixed with a few protons, and then the seed nuclei had to be built up from this starting point. But just below the surface of the neutron star the abundance distribution should look like that in Figure 5. In view of quasiadiabatic cooling in the expansion of this material, particularly as heating due to the neutrino-antineutrino flux declines, it is not clear that these potential seed nuclei will be eliminated as the material passes through lower densities. If that is the case, then neutron capture would be able to move such nuclei in the direction of the next closed neutron shell of 82 neutrons (to mass numbers near 132). And the buildup of lighter seed nuclei in the manner of Hoffman, Woosley, and Qian (1997) would produce r-process nuclei in the range up to mass numbers of 80 or 90. These possible processes need to be examined in some detail, as winds emitted from the polar regions of nascent neutron stars could therefore account for the r-process nuclei below A = 90, the r-process in the extrusion disk could account for the r-process nuclei above A = 132, and both processes could contribute to the r-process nuclei in the intermediate region. The entire region below A = 132 may be sensitive to the precise collapse dynamics of presupernovas of different masses, where the r-process abundances are observed to be variable among ultra-metal-poor stars. The abundances above A = 132 are much more relatively constant, which would imply that the extrusion disk phenomena are less mass sensitive. G. J. Wasserburg, M. Busso, and R. Gallino (1996) suggested that there must be two separate types of r-process for these regions. This scheme would provide them both as distinct processes in core collapse supernovas.

I now turn to some discussions about other aspects of this scenario that may tend to validate it. When the jets are initially launched, the first thing they

Spallation in the Expanding Envelope

- **The jets will run into the expanding supernova envelope. The main effect will be to slow the energetic nuclei to rest relative to the envelope, but at 140 MeV per nucleon there will be a great deal of spallation. Both the target nuclei in the envelope and the projectiles themselves will undergo spallation. There will be observable nucleosynthesis consequences of this. Hence I call these nucleosynthesis effects the c-process (for "collisional").**

- **The total kinetic energy in the jets will be 5×10^{48} ergs or perhaps considerably more. Although much of the kinetic energy of the jets may not be expended in the envelope but in blasting a hole through it, a substantial secondary explosion will occur. This will spread the products carried in the jets over much larger solid angles than subtended by the jets themselves. Nevertheless the r-process and c-process products will be strongly concentrated in the jet directions, while the explosive burning products of the supernova will be much nore nearly isotropically distributed (i.e., the [Eu/Fe] ratio will be highly variable).**

- **Light Nuclei: The c-process will produce interesting consequences in the Carbon-Oxygen region of the supernova and also in the Helium region. The spallation products will include the Li, Be, and B isotopes in the Carbon-Oxygen region and deuterium, tritium, and ^{3}He from both regions. These are all nuclides that conventional wisdom says willl not be produced in stellar interiors. If the presupernova has a hydrogen outer shell and free neutrons are carried up in the jet (and have not already diffused out of it), then this will be an additional source of deuterium. An interesting question is whether these c-processes contribute more of less of these products to the interstellar medium than the cosmic ray spallation.**

Viewgraph 6

---

must do is to punch holes through the expanding supernova envelope. With a velocity of $0.5c$, they will very quickly overtake the envelope, which will

be travelling at of order 10^9 cm/sec, although the total outward motion of the envelope may not have become organized at the time under consideration. This does not matter because the motions are slow compared to those in the jets. The total kinetic energy in the jets is about 5×10^{48} ergs or possibly considerably more. If all of this were to be thermalized in the collision between the jets and the envelope, then this would cause a very substantial secondary explosion within the supernova envelope, but it would not be generally observable as a separate event from afar. However, the early material in the jet is likely to blast open a path through the envelope that will allow the later material to pass through and to let the deexcitation gamma rays be emitted in a forward beam, so that the energy in the secondary explosions in the envelope will be less than the total thermal energy in the jets. This assumes that there is not still an extensive outer hydrogen layer in the envelope, since the time scale for most of the gamma ray emission would then become smaller than the total penetration time. See Viewgraph 6.

The actual development of the collision is likely to involve the heavy ions smashing through the envelope for the most part, leaving a trail of ionization along a cylindrical path within the envelope similar to that left by a heavy cosmic ray ion traversing a nuclear emulsion. Most ions would not make a nuclear collision with another nucleus in the envelope, but a substantial number would do so, and the earlier ions in the jet should be slowed down to rest in the envelope, as a cylindrical path in the envelope is energized. This cylinder will then expand laterally (but the fluid will have acquired a substantial forward motion as well), and thus a cylindrical shock wave will be launched. This will be the process that distributes r-process and other nuclei over a larger solid angle in the vicinity of the supernova, despite the narrowness of the r-process jets. However, this will still leave the distribution of r-process nuclei ejected from the supernova having relatively narrow peaks that fan out away from the jet direction.

Even though most of the nuclei in the jet will not cause nuclear reactions in the envelope, a substantial number will do so. The products of such nuclear spallation will tend to lie on the neutron deficient side of the valley of beta stability when the spalled nucleus is in the envelope, but the spallation of r-process products can still leave neutron-rich nuclei behind, particularly if the ion has substantially slowed down before making the nuclear collision. Thus such spallation events can cover the range from neutron-rich to neutron-poor nuclei, thus overlapping the production of r-process, s-process, and p-process

nuclei. I am calling this the c-process (for collisional). Since the p-process nuclei tend to have much smaller abundances than the other types, it is among these that the effects due to the c-process are most likely to be found.

We have learned a lot about the r-process from the study of the abundances of the elements in ultra-metal-poor stars. The heavier elements in such stars, which in general tend to have abundances only about 10^{-3} of solar, appear to be solely made by the r-process, with s-process products becoming mixed in when the abundance level rises to about 10^{-2} of solar. It is thus particularly noteworthy that there can be large variations in the ratio of r-process elements to lighter ones such as iron. A particularly extreme case exists in the star CS 22892-052, shown in Figure 11. Here the abundances of elements with Z $\sim$ 70 are about a factor 30 more abundant than iron, as compared to the Sun, in which they are typically more like six orders of magnitude less abundant than iron. This kind of enrichment would be possible if a supernova occurred in a fairly massive primordial stellar cluster, and some of the gas there received an injection of material directly from an r-process jet.

Of course such extreme cases are unlikely to be seen at later stages of galactic evolution when the element abundances in a given patch of gas represent an average of many stars. Nevertheless one should expect greater variations at earlier times in the galaxy when fewer stars contribute to the average, and this is seen in Figure 12, in which the abundance of Eu (a convenient r-process marker) is compared to the abundance of Fe, as a function of Fe/H, and hence of galactic age. Note that the scales are plotted logarithmically. The downturn at late galactic ages in Figure 12 is due to the fact that Fe production in the early universe is due to core-collapse supernovas, whereas later there is an additional production due to Type Ia supernovas that take longer to evolve because they are produced when white dwarfs accrete matter from a binary companion.

I now discuss the very earliest generations of primordial stars in the light of the above results. Before there were any products of stellar nucleosynthesis present in the interstellar medium (just the very lightest isotopes due to big bang nucleosynthesis), the gas lacked efficient cooling mechanisms, and consequently it was difficult for it to fragment into low mass stars. Hence the very first generation of stars is expected to have consisted solely of very massive stars, mostly several hundred to a thousand solar masses, and perhaps extending down to a few at about 30 solar masses. The evolution of such stars has been calculated by Heger and Woosley (2002). What they found (Figure 13)

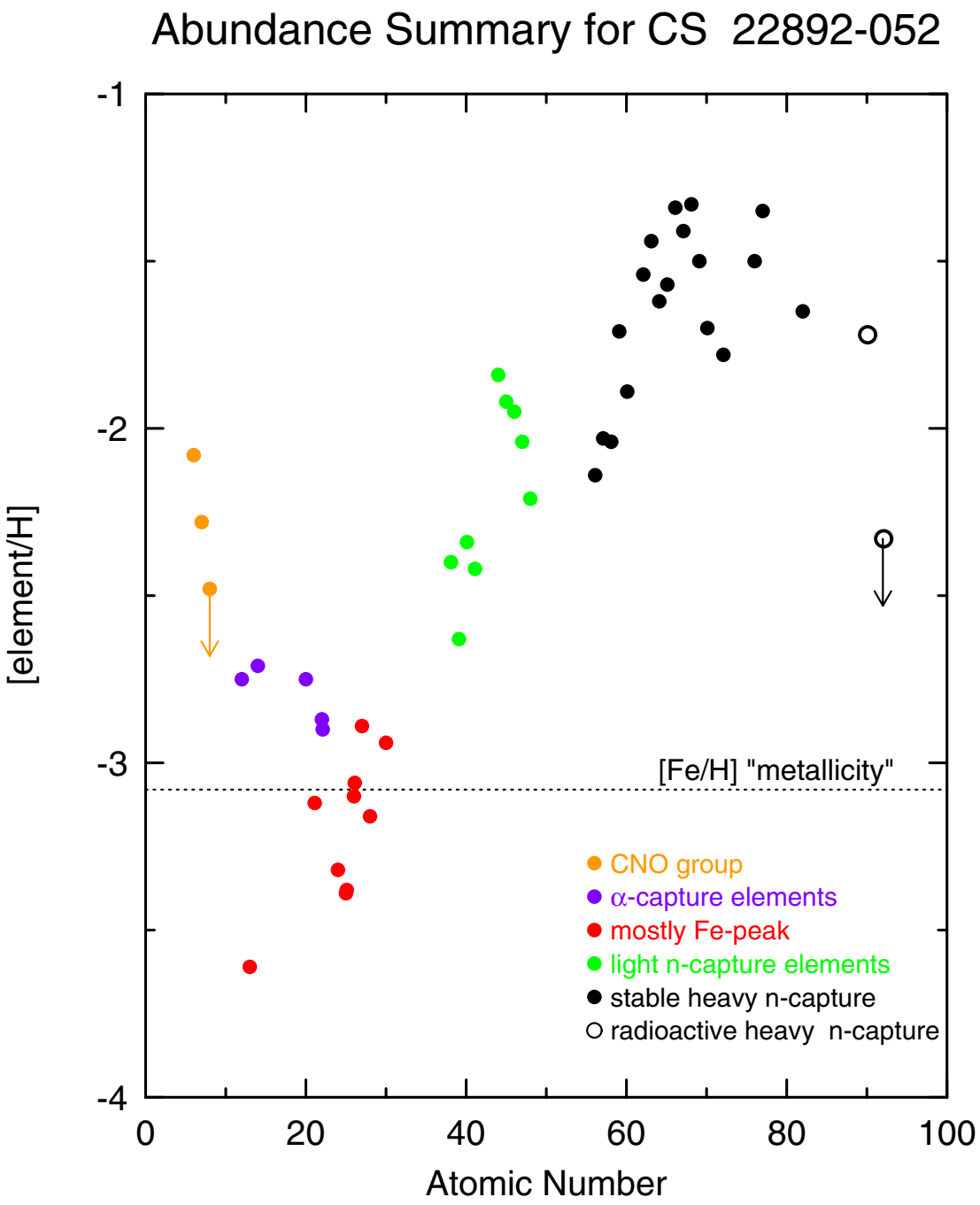

Figure 11. Extreme abundance anomalies in an ultra-metal-poor star. Courtesy of C. Sneden and J. Cowan.

was that in the mass range below 140 $M_{\odot}$ the stars evolve to the supernova

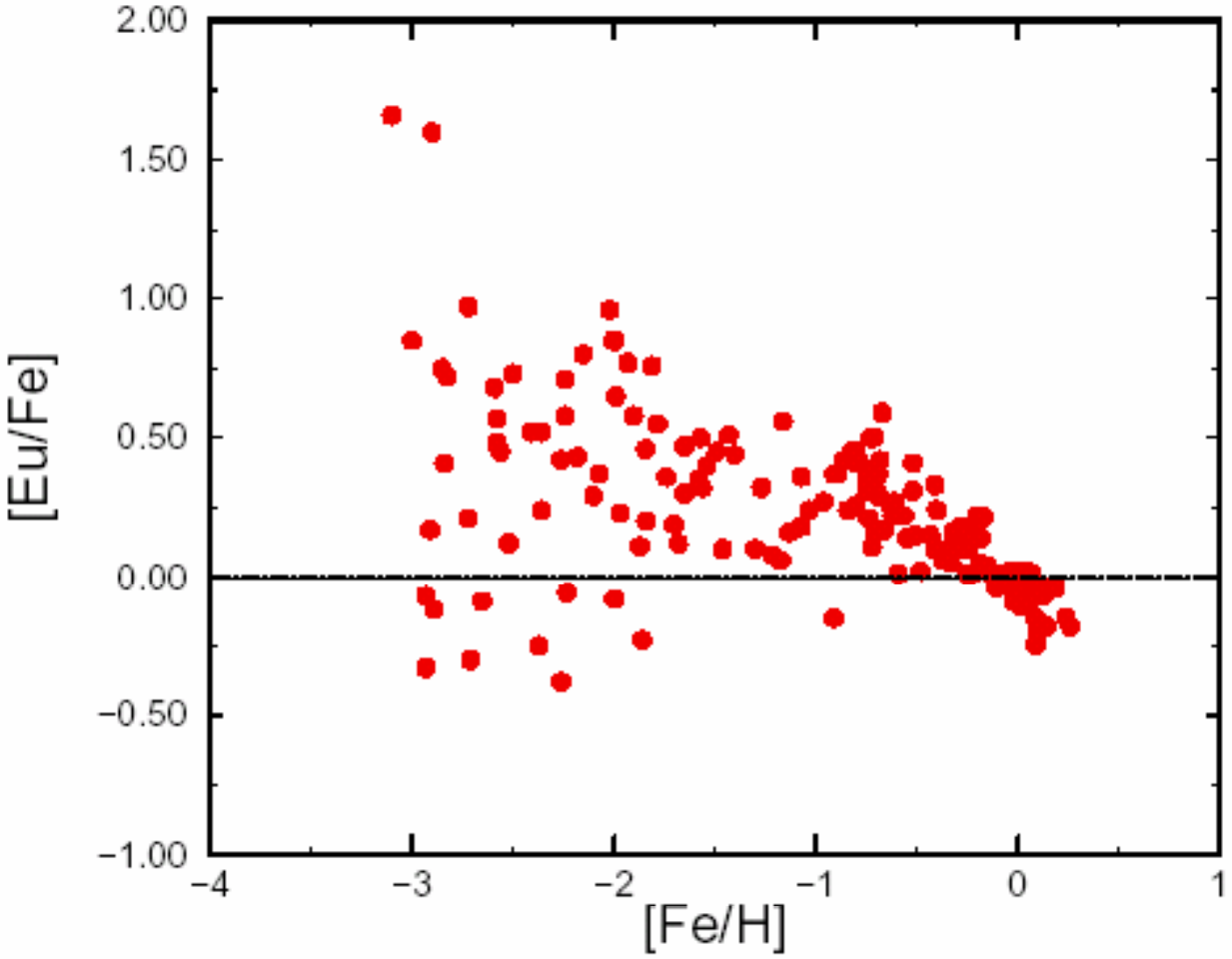

Figure 5: The ratio [Eu/Fe] is displayed as a function of [Fe/H] from various surveys of halo and disk stars as detailed in (*11*). The dotted line represents the solar value.

Figure 12. A measure of the variable ratio of r-process to iron production as a function of galactic evolution. Courtesy of C. Sneden and J. Cowan.

---

stage and leave behind black holes. From 140 to 260 $M_\odot$ the stars undergo an electron-positron pair instability that results in a greater than normally energetic supernova explosion and the stars are completely disrupted. They distribute intermediate mass elements into the interstellar medium (Figure 14). The mass range above 260 $M_\odot$ collapses directly to black holes. Since the bulk of the mass is expected to lie in this mass range, it means that something of the order of 80 per cent of the initial baryonic mass in the universe is promptly swallowed up in black holes.

This gives a very satisfactory picture for the mass content of the universe.

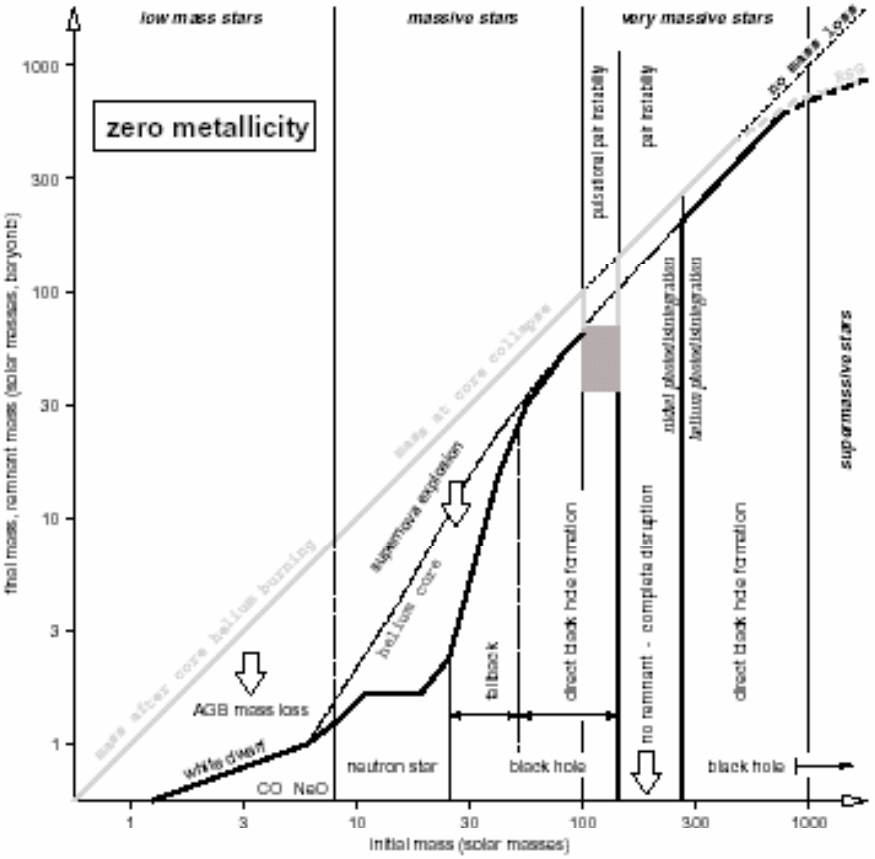

FIG. 2.—Initial-final mass function of nonrotating primordial stars ($Z = 0$). The x-axis gives the initial stellar mass. The y-axis gives both the final mass of the collapsed remnant (*thick black curve*) and the mass of the star when the event begins that produces that remnant (e.g., mass loss in AGB stars, supernova explosion for those stars that make a neutron star, etc.; *thick gray curve*). We distinguish four regimes of initial mass: low-mass stars below $\sim 10\,M_\odot$ that end as white dwarfs; massive stars between ~ 10 and $\sim 100\,M_\odot$; very massive stars between ~ 100 and $\sim 1000\,M_\odot$; and supermassive stars (arbitrarily) above $\sim 1000\,M_\odot$. Since no mass loss is expected for $Z = 0$ stars before the final stage, the gray curve is approximately the same as the line of no mass loss (*dotted line*). Exceptions are ~ 100–$140\,M_\odot$, where the pulsational pair instability ejects the outer layers of the star before it collapses, and above $\sim 500\,M_\odot$, where pulsational instabilities in red supergiants may lead to significant mass loss (Baraffe et al. 2001). Since the magnitude of the latter is uncertain, lines are dashed. In the low-mass regime we assume, even in $Z = 0$ stars, that mass loss on the AGB leads to the star losing its envelope and becoming a CO or NeO white dwarf (although the mechanism and thus the resulting initial-final mass function may differ from solar composition stars). "Massive stars" are defined as stars that ignite carbon and oxygen burning nondegeneratively and do not leave white dwarfs. The hydrogen-rich envelope and parts of the helium core (*dashed–double-dotted curve*) are ejected in a supernova explosion. Below an initial mass of $\sim 25\,M_\odot$, neutron stars are formed. Above that, black holes form, either in a delayed manner by fallback of the ejecta or directly during iron core collapse (above $\sim 40\,M_\odot$). The defining characteristic of *very* massive stars is the electron-positron *pair instability* after carbon burning. This begins as a pulsational instability for helium cores of $\sim 40\,M_\odot$ ($M_{\rm ZAMS} \sim 100\,M_\odot$). As the mass increases, the pulsations become more violent, ejecting any remaining hydrogen envelope and an increasing fraction of the helium core itself. An iron core can still eventually form in hydrostatic equilibrium in such stars, but it collapses to a black hole. Above $M_{\rm He} = 63\,M_\odot$ or about $M_{\rm ZAMS} = 140\,M_\odot$, and on up to $M_{\rm He} = 133\,M_\odot$ or about $M_{\rm ZAMS} = 260\,M_\odot$, a single pulse disrupts the star. Above $260\,M_\odot$, the pair instability in nonrotating stars results in complete collapse to a black hole.

Figure 13. The results of Heger and Woosley on the end-points of evolution of the first stellar generation of massive stars (from about 30 $M_\odot$ to about 1000 $M_\odot$. Only the stars from about 140 $M_\odot$ to about 260 $M_\odot$ are expected to produce heavier elements for incorporation into the second stellar generation; the rest of the stars with most of the total mass are expected to form black holes.

Of order 80 per cent of this mass forms what is known as dark matter. It is often suggested that this consists of unknown hyperonic or other strange type of species, but it is much more satisfactory to identify it with these black holes.

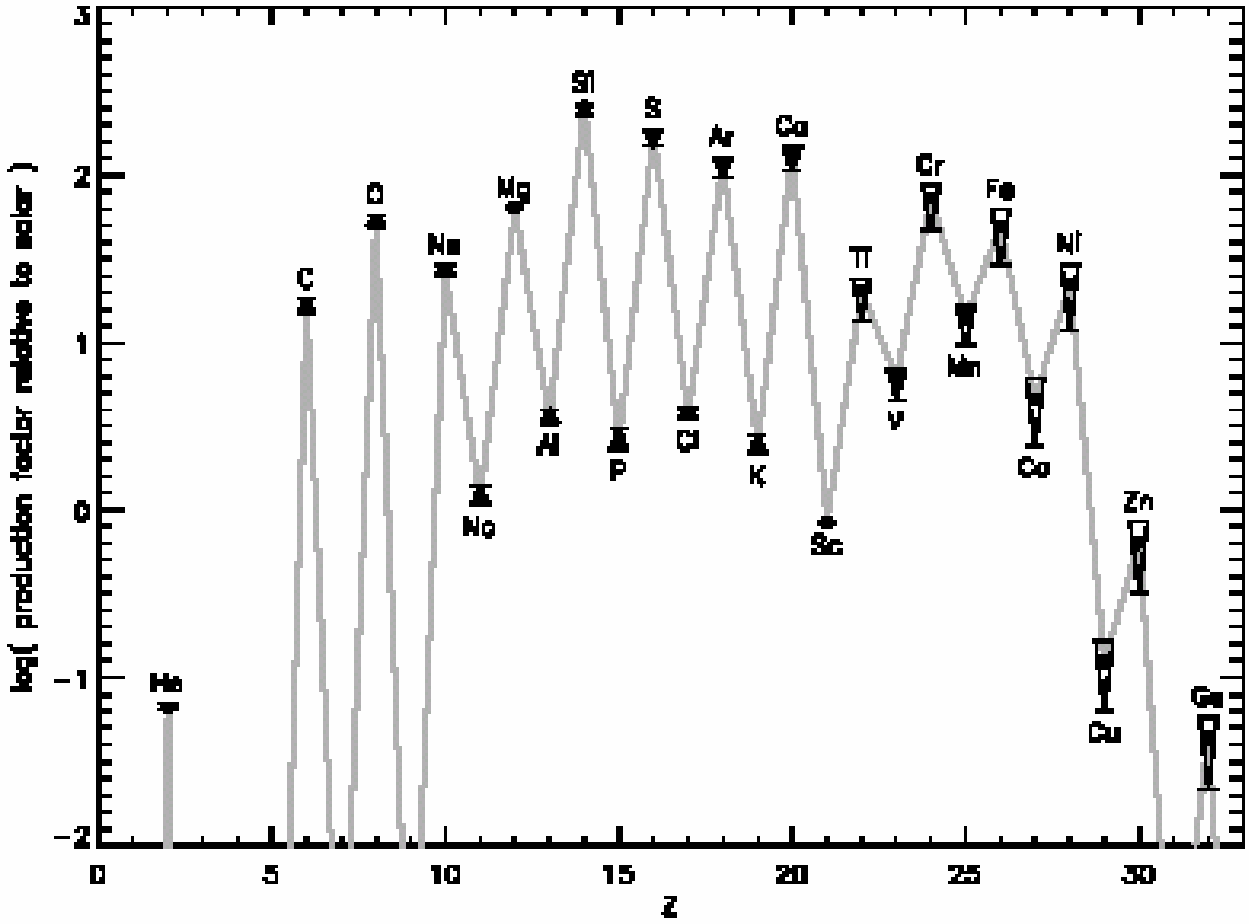

FIG. 3.—Production factors for very massive stars (helium cores of 65–130 $M_\odot$, corresponding to initial masses of $\sim$140–260 $M_\odot$) integrated over an IMF and compared to solar abundances as a function of element number Z. The integration assumed a Salpeter-like IMF with three different exponents: -0.5 (*thick end of triangle*), -1.5 (*solid dot*), and -3.5 (*thin end of triangle*).

Figure 14. The element distribution that should exist in the second generation of primordial stars. From Heger and Woosley.

When black holes find themselves within galaxies, in the higher density regions stellar gravitational friction will cause them to spiral into the center and merge to form the central black holes (and quasars) that typically have millions of solar masses (Schneider *et al.* 2002). The same thing can happen in the globular clusters where the black holes can have thousands of solar masses. But the large galaxies form by mergers of many smaller ones, and these galaxies will

bring many additional black holes into the bigger ones. The smaller galaxies are tidally disrupted, leaving their black hole components on the original infall trajectories. In general it will take a long time for such highly elliptical orbits to decay by stellar gravitational friction, so that the orbits will stick out well into the intergalactic medium. This places a very large mass component into extended galactic halos, which is where most of the massive dark matter lies. There is no demonstrated need for unknown species. Nevertheless, this unseen mass component constitutes a potential hazard to the future of the human race.

The nucleosynthesis products of the first stellar generation provide the gas with a larger range of cooling agents, and hence the gas can fragment into smaller pieces when it forms the second generation of stars. These should evolve much more normally to be able to form standard core collapse supernovas, and hence to leave behind neutron stars. The mechanismss described here should then be able to operate on the nascent neutron stars, producing r-process products, and hence stars with a prominent r-process abundance distribution should become part of the third and subsequent generations of stars.

There is indeed an effect in the p-process abundances that can be attributed to the c-process. Figure 15 shows a plot of total nuclidic abundances according to the Anders-Grevesse (1989) table, together with their p-process component. It is striking that at A = 90 there is a peak in the p-process abundances that makes them comparable to the s-process component there. The calculations of Rayet *et al.* (1995) reproduced the p-process abundances very well everywhere except at this A = 90 peak, where the abundances were grossly underproduced. However, note that Figure 5 shows a sharp peak at A = 90, due to nuclear statistical equilibrium at lower densities where the r-process has not operated. I have already noted that this lower density material will exist in the accretion disk flow to the roots of the jets, and hence it will participate in the spallation processes in the expanding envelope. Such spallation reactions need not, on average, significantly diminish the mass number of the bombarding nuclei, since collisions with He, C, and O can add nucleons as well as simply subtracting them.

Thus, in Figure 16 I show an enlargement of the area around A = 90 in both the Anders-Grevess table and the p-process component. I also show the peak of the nuclear statistical equilibrium calculation in Figure 5 and a modification of it in which I have eliminated the shell and pairing corrections from the

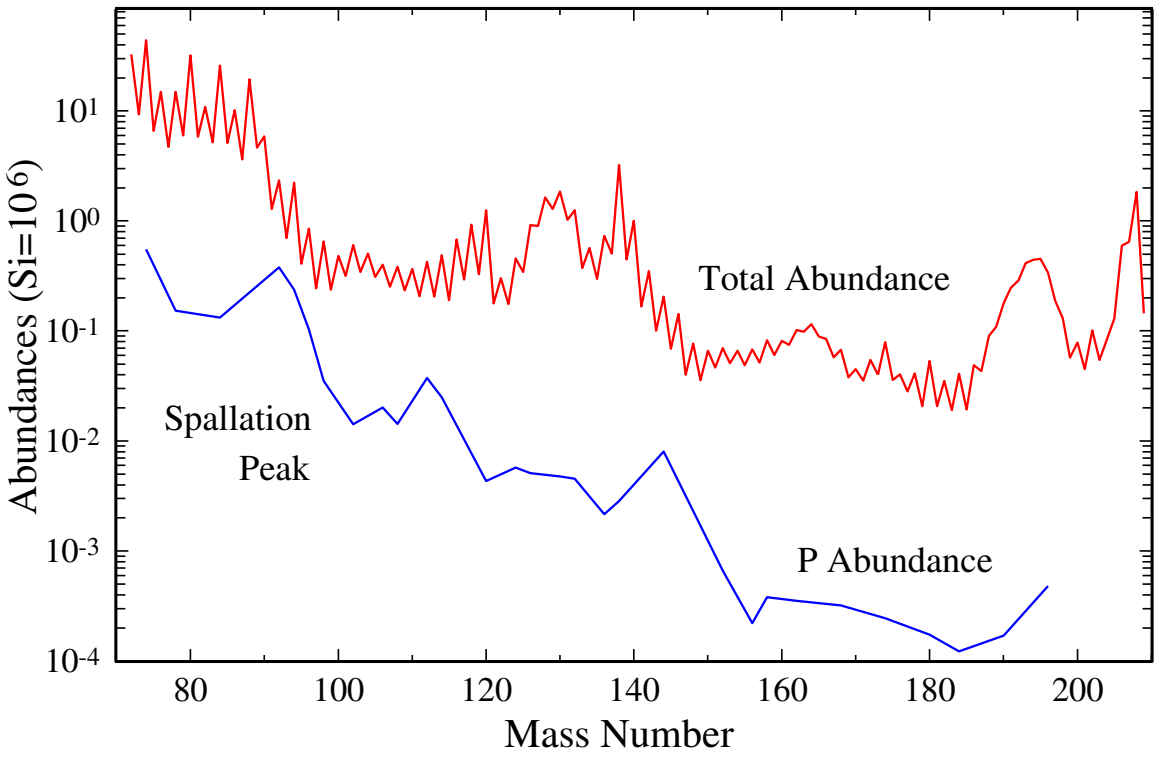

Figure 15. The Anders and Grevesse abundance distribution of the nucides (on top) and the p-process component of it below. Note the hump in the p-proces values in the mass number 90 to 100 region.

---

mass formula used in calculating (but not in the nuclear level density parameters used there). Since shell corrections tend to diminish as one approaches the neutron drip line, the correct nuclear equilibrium distributions probably lie between these curves. These calculations may be considered to complement those of Rayet *et al.*.

Next we consider the isotopic anomalies associated with Te and Xe extracted from interstellar nanodiamonds found in carbonaceous meteorites. The Xe is obtained by heating, and different components come out at different temperatures. One of these is the Xe-HL component that appears to have been a pure supernova contribution to the nanodiamonds. Another component, Xe-P3, is believed to represent normal Xe (Huss and Lewis 1994). Figure 17 shows the ratio of the abundances of these isotopic components, a characteristic bowl-shaped

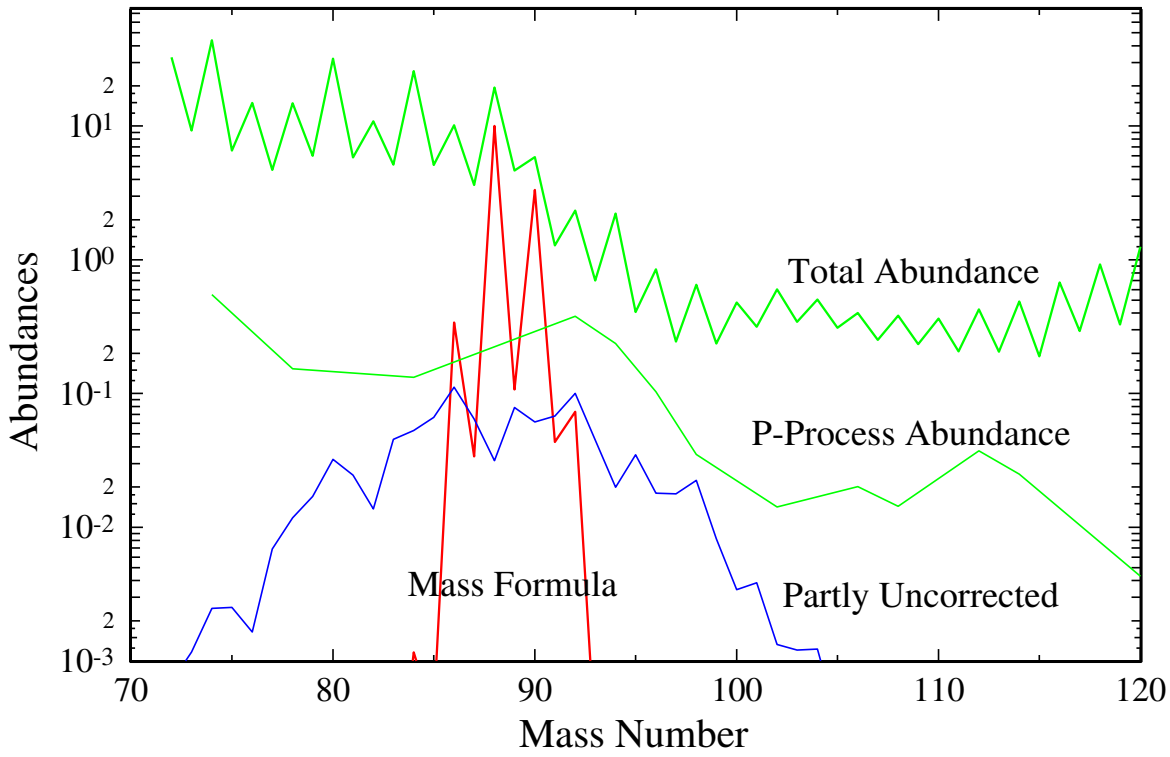

Figure 16. The upper jagged line shows the total Anders-Grevesse nuclide abundances plotted as a function of mass number, and below that line is a second line showing the abundances of the p-process nuclei in the Anders-Grevesse table. The narrow spallation peak is the equilibrium abundance distribution as given in Figure 5, arbitrarily normalized in the plot. For comparison, the broader curved distribution is the equilibrium peak with shell and pairing corrections removed (but not the shell and pairing corrections to the level densities, to which the equilibrium abundances are less sensitive.

---

diagram that has mystified meteoriticists for many years. The Te-H component is normal except for excesses of the two heaviest isotopes. But this apparently makes more sense when the absolute differences are plotted, as in Figure 18, in which the two anomalous Te-H isotopes have been normalized to Xe-HL so as to lie on the slope of the line passing through the Xe isotpes at A = 132 and 134. This Xe-H curve appears to be the lower side of the fission fragment curve tentatively assigned to the fisson of ^{297}Bh. Parallel to this line are additional lines

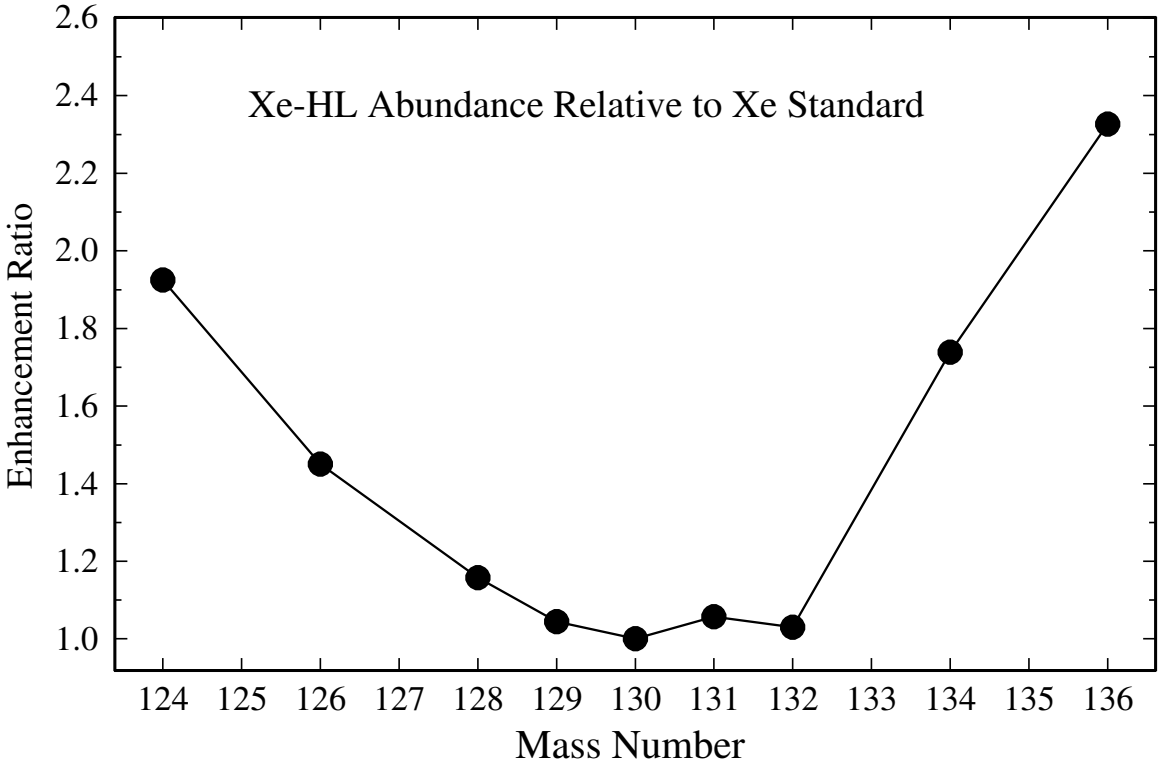

Figure 17. A plot of the ratios of the isotope abundances for Xe-HL relative to a normal xenon abundance distribution taken as the Xe-P3 distribution of Huss and Lewis, for xenon extracted from meteoritic nanodiamonds. This is the normal presentation of the Xe-HL pattern but with a simplified notation. The distributions have been renormalized to ^{130}Xe rather than to the original normalization to ^{132}Xe.

differing from it by the loss of one or more neutrons. These appear to identify the anomalous abundances of Xe-L as being spallation products of the fission xenon peak.

Now I turn to some of the isotopic anomalies in the solar system. The most prominent of these are the extinct radioactive nuclides whose excess decay products are found in meteoritic material. There are a little more than a dozen of these, corresponding to half-lives of about 10^5 to a little over 10^8 years. A few of them are r-process products. The only stellar sources that can produce all of these are core collapse supernovas. See Viewgraph 7. The picture that has

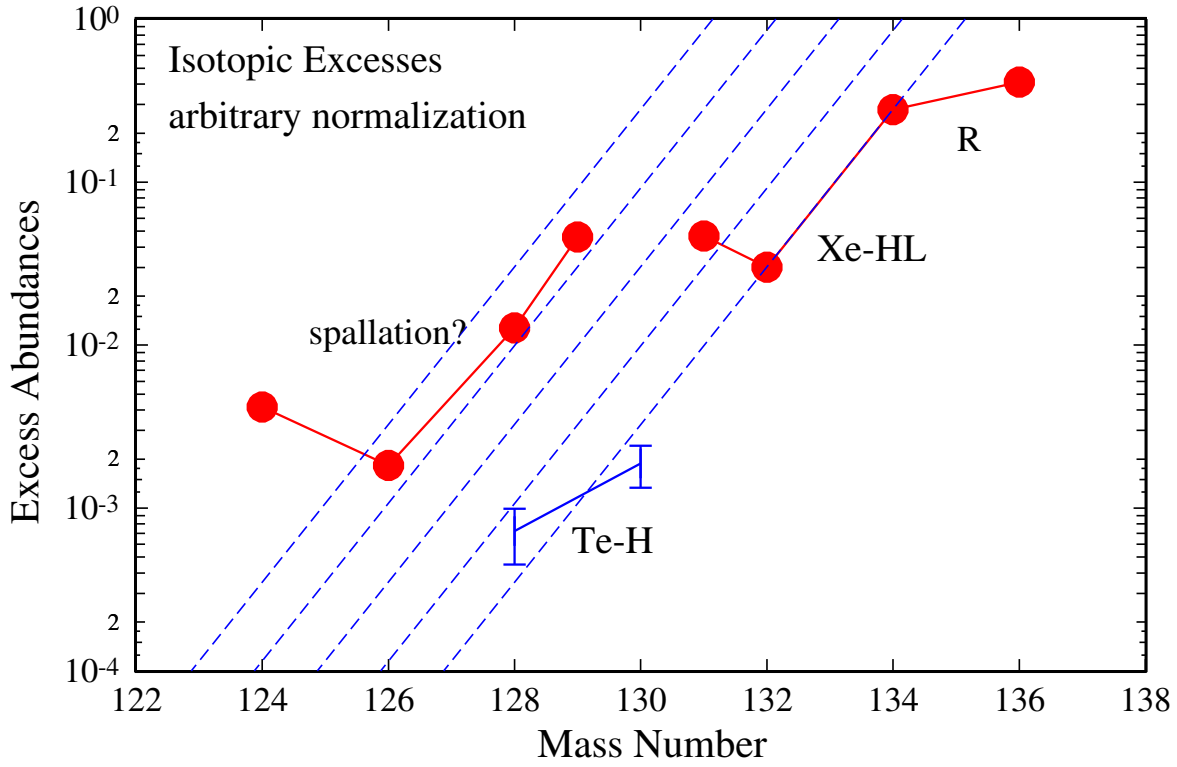

Figure 18. A replot of Figure 15 to show the absolute values of the abundance differences between the renormalized Xe-HL and Xe-P3 distributions. ^{130}Xe is not plotted since it is the base of the renormalizations and its abundance difference is unknown; if it were known the Xe-HL points would be slightly raised. Also the abundance excesses of Te-H extracted from interstellar nanodiamonds are plotted with arbitrary normalization such that the projection of the Xe-HL line that joins mass numbers 134 and 132 passes between the two Te-H points. The hypothesis is made that the Xe abundances below A = 132 have resulted from spallation of the r-process abundance distribution in the collision between the r-process jets and the expanding supernova envelope. I have assumed that the lower slope of the rising abundance peak is given by a projection of the line joining ^{134}Xe and ^{132}Xe, and a line is drawn to show this. This line is repeated on the left to show successive removals of evaporated neutrons by spallation excitation.

---

emerged is that when such a supernova is formed in a young stellar association

in a molecular cloud complex, it will explode within a few parsecs of a number of molecular cloud cores. When the supernova shock wave arrives at such a core, it will compress it into accelerated collapse and introduce fresh radioactive species into the resulting primitive stellar nebulas (simulations of this process have been made by Vanhala and Cameron (1998) and by Vanhala and Boss (2002)). Figure 19 shows the simulation of the injection process by Vanhala and Boss; the interface is unstable against the development of Rayleigh-Taylor fingers, and the injection efficiency for bringing the radioactivities into the interior is about ten per cent.

A particularly important recent discovery was the presence in meteoritic materials of the ^{7}Li decay products of the nucleus ^{7}Be, which has a half life of only 53 days. This was found in a meteoritic calcium-aluminum inclusion (CAI), a class of macroscopic object which typically has dimensions of about a millimeter to about a centimeter or a bit more. Such objects are the first significant condensates to be formed in a cooling gas of solar composition. In this the abundance of ^{7}Li was variable over a distance of order 50 μm, and these variations were correlated with similar variations in ^{9}Be. Now 53 days is a minute speck of time in comparson to the lifetime of the primitive solar nebula, and the injection process from the supernova would also take many orders of magnitude longer than this half life. So it makes more sense to attribute the formation of CAIs to the expanding supernova envelope. Isotopes such as ^{7}Be are of course products of the spallation c-process, in this case taking place when the r-process jet traverses the carbon-oxygen and helium-burning layers in the supernova envelope. I attribute the variability of the ^{7}Be abundance to condensation of different parts of the CAI at different places, followed by mutual collisions and fusion into the larger CAI itself. I also infer that the medium was turbulent in order to promote these collisions.

Now the CAIs have a fairly uniform enrichment of pure ^{16}O at the level of 4 to 5 percent relative to ^{17}O and ^{18}O, which have a normal ratio. From this I infer that the supernova envelope had been subject to large-scale mixing, in which products of the carbon-oxygen layer (which has pure ^{16}O) have been spread around to the other layers. This is consistent with the previous inference of the presence of turbulence.

There are numerous other isotopic anomalies in meteorites that can be attributed to the supernova environment. There are other types of inclusions including amoeboid olivine aggregates (AOAs) composed of magnesium and iron

The Supernova Trigger for the Solar System

- **There are many extinct radionuclides that have left traces of their decay in primitive solar system material. These include r-process nuclides such as ^{129}I, ^{182}Hf, and ^{244}Pu. The only astronomical object that can produce all of these is a core collapse supernova. Hydrodynamic simulations have shown that a supernova shock wave propagating in a molecular cloud can trigger the collapse of the core at distances of 4 to 10 parsecs. The extinct radioactivities are injected into the collapsing core via Rayleigh-Taylor fingers at the interface.**

- **Recently discovered extinct radioactivities are ^{7}Be and ^{10}Be with half lives of 53 days (!) and 1.5 million years, respectively. The decay products with excess abundances are ^{7}Li and ^{10}B, and these are found in meteoritic calcium-aluminum inclusions (CAIs) with variations over distances like 50 μm. Abundance variations are correlated with those of ^{9}Be. I interpret this to mean that the CAIs were not formed in the solar nebula but in the expanding envelope of the triggering supernova, where the expansion time scale is comparable to the half life of ^{7}Be. They would be injected into the molecular cloud core at the same time as the other extinct radioactivities.**

- **In the presupernova core collapse neutrino heating creates huge bubbles that induce mixing in the supernova envelope (SN1987A emitted gamma rays months earlier than expected). The CAIs rather uniformly have excess abundances of ^{16}O of 4 to 5 percent, which would be due to mixing of the carbon-oxygen zone throughout the envelope. Amoeboid olivine aggregates (AOAs, Mg and Fe silicates) are condensates formed subsequent to CAIs, and share this ^{16}O anomaly. Meteoritic matrix material contains huge amounts of nanodiamonds, formed from the incomplete helium burning region of the presupernova; among several types of material extractable by stepwise heating appear to be Xe isotopes formed by a pure r-process as well as by the c-process operating on the energetic Xe nuclides in the jets. There are many types of presolar grains with isotopic anomalies in several elements that can be interpreted in similar ways.**

Viewgraph 7

---

silicates that would condense at lower temperatures than the CAIs, and which also share an enrichment of pure ^{16}O at the level of 4 to 5 per cent. The inter-

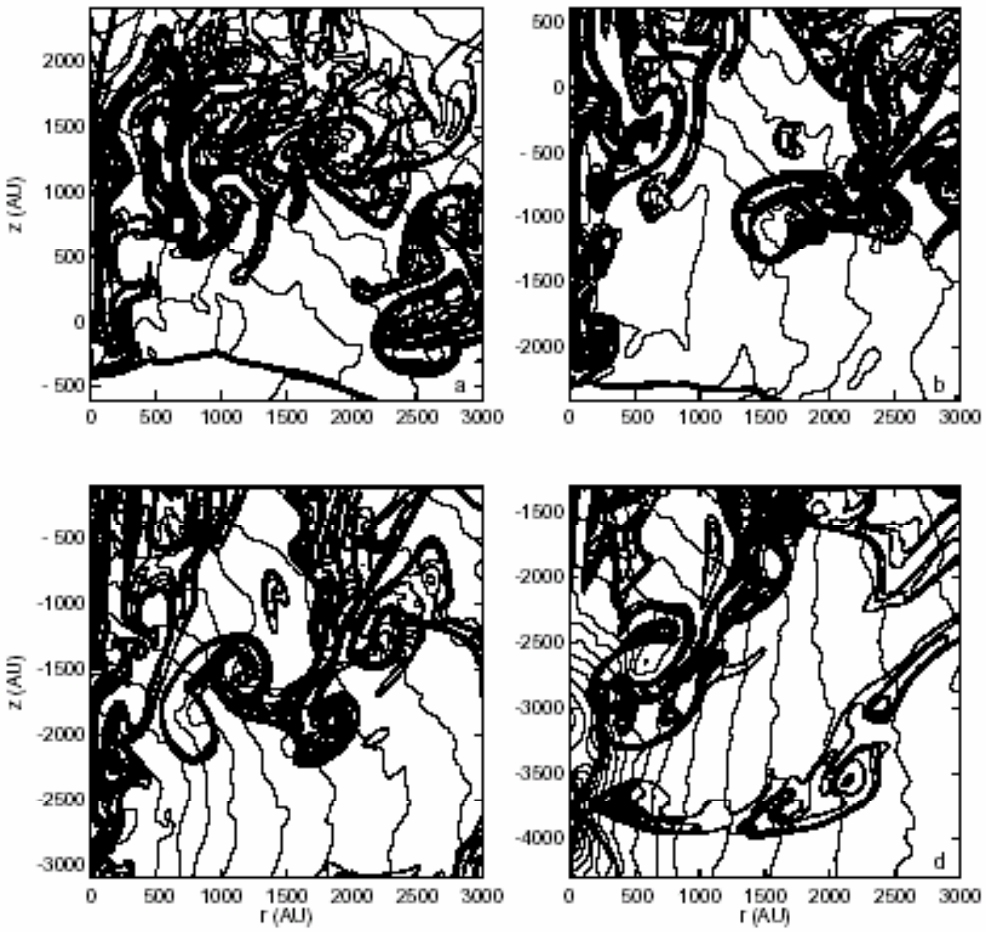

FIG. 2.—Close-up of the R-T fingers. The system is shown at (*a*) $t = 66,000$ yr, (*b*) 88,000 yr, (*c*) 110,000 yr, and (*d*) 132,000 yr. The thin contours depict the gas density in the system and range from 6.20×10^{-21} to 7.93×10^{-16} g cm^{-3}, with each contour representing a change of factor 1.5 in density. The thick contours show the behavior of the color field and range from 0 to 3.40×10^{-20} g cm^{-3} in steps of 2.43×10^{-22} g cm^{-3}.

Figure 19. Triggered formation of the solar system. This figure shows the Rayleigh-Taylor fingers developed as the incident supernova shock wave impacts on a molecular cloud core, mixing supernova ejecta into the core interior. From H. Vanhala and A. Boss.

stellar nanodiamonds are likely to be formed in the expansion of the region of the supernova containing incomplete helium burning products, which is rich in carbon. There are many different kinds of presolar grains, some of which are attributed to supernova production. All of these effects are likely to be useful probes of the supernova envelope.

Why does this mixing occur in supernova envelopes? The first hint of it came with the outburst of SN 1987A, when gamma rays were detected several months before they were expected. The recent 3D simulations of the collapse of a presupernova core are instructive in this regard. These have been carried out at Los Alamos by Chris Fryer, Mike Warren, and colleagues. Figure 20 shows the

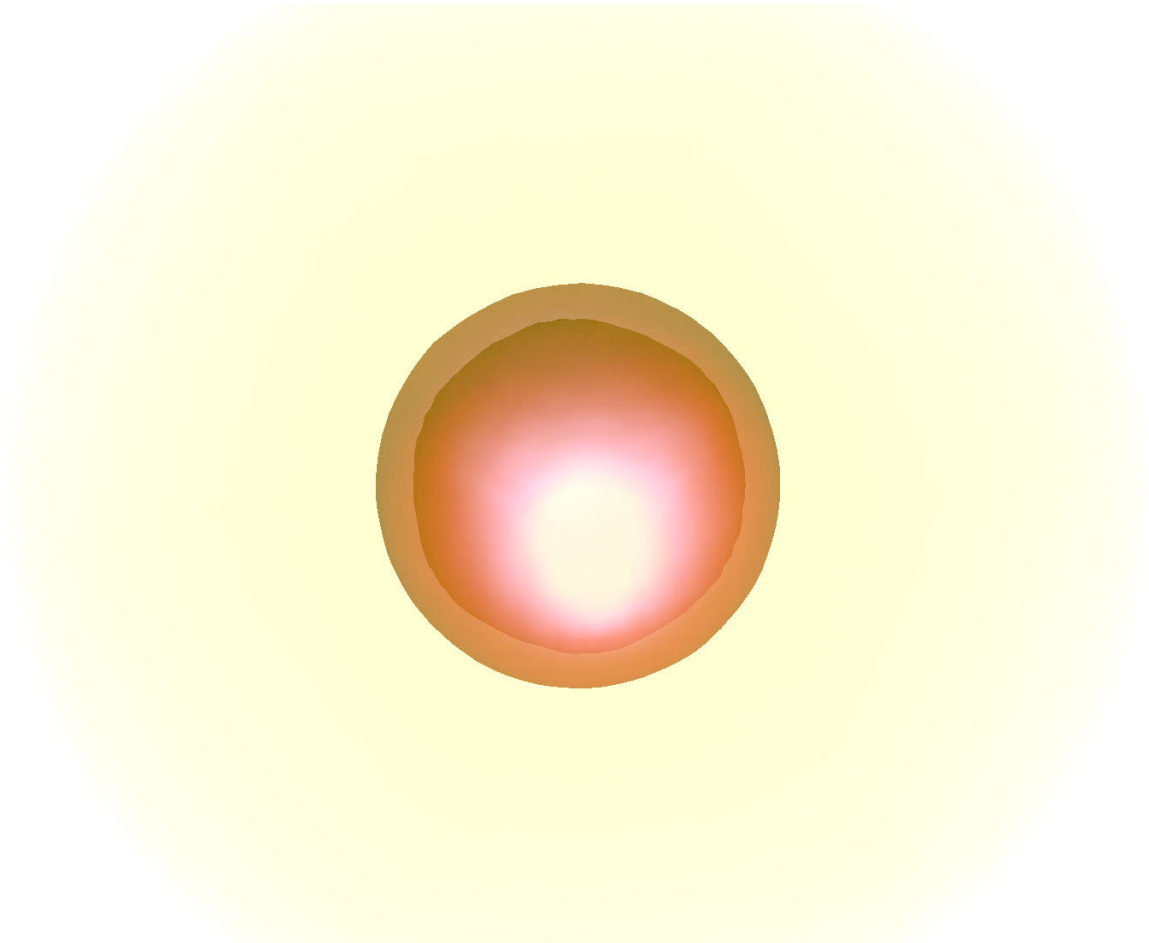

Figure 20. Three-dimensional simulation of a core-collapse supernova in the collapse phase. From Los Alamos press release.

---

core collapsing. Figure 21 shows the kind of circulation patterns that develop in the core. Here there are currents of cool matter falling into the center, where they are heated by the neutrinos and antineutrinos generated there. From these, bubbles develop much like vigorously boiling water in a saucepan, except that there the heating is at a two-dimensional surface, whereas in the supernova the heating is from a point source. Figures 22 and 23 show the development of these bubbles. The highly anisotropic nature of these bubbles, expanding faster than the surroundings, not only develops into internal shocks within the supernova interior, but also is very effective in stirring up the interior.

References

E. Anders and N. Grevesse, Geochim. Cosmochim. Acta, **53**, 197 (1989)

W. Baade, The Observatory, *77*, 165 (1957)

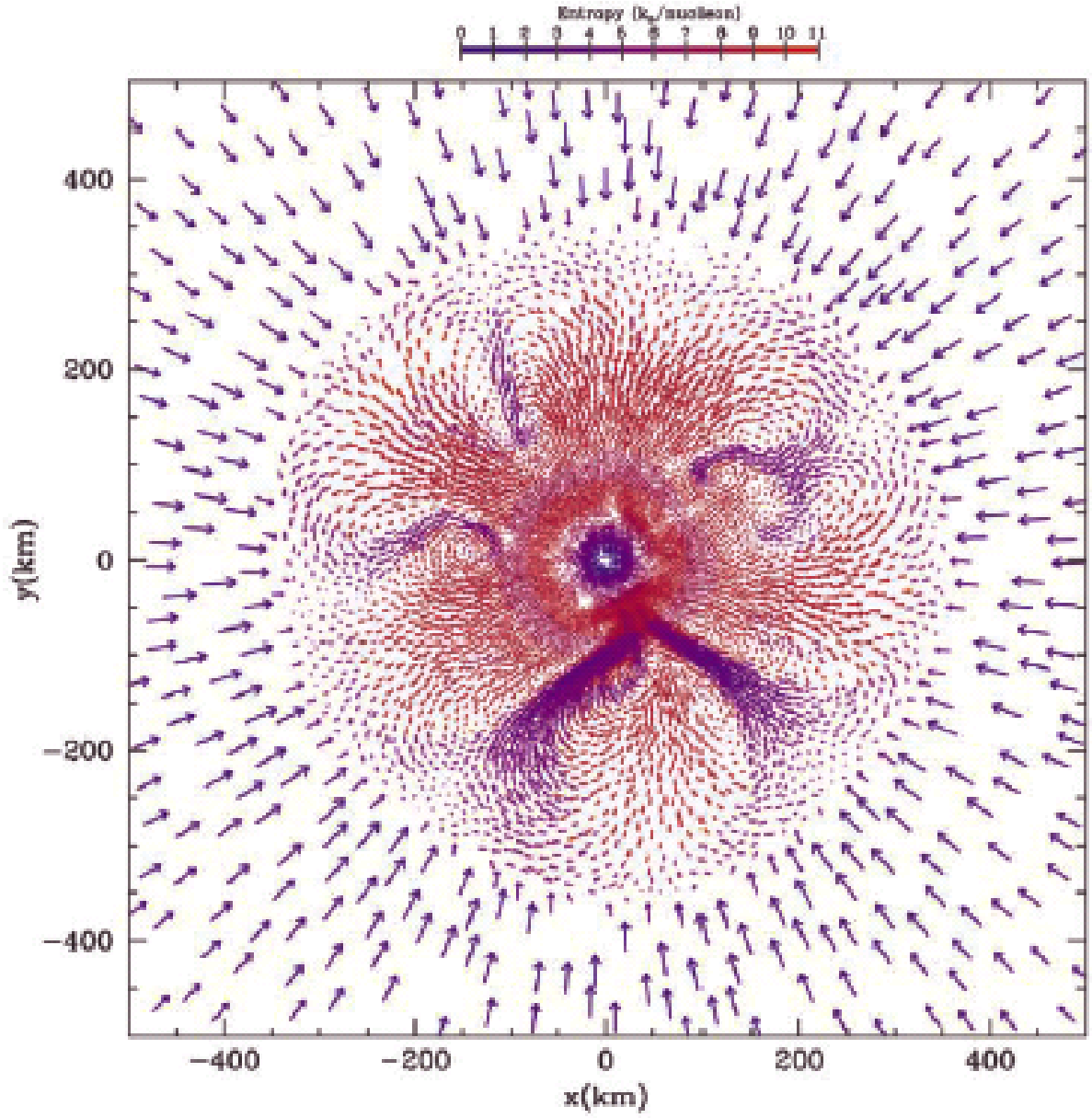

FIG. 2.—Slice of model B, colored by its entropy and showing velocity vectors. The cold, low-entropy material flows downward as the high-entropy material bubbles upward. Note that the size scale and even structure of this convection is very similar to two-dimensional models (see Herant et al. 1994; Fryer 1999).

Figure 21. Mixing in core of a supernova in 3D simulation. Cold currents descend toward the center, are heated by neutrinos and antineutrinos, forming hot bubbles that rise and expand. From Fryer and Warren.

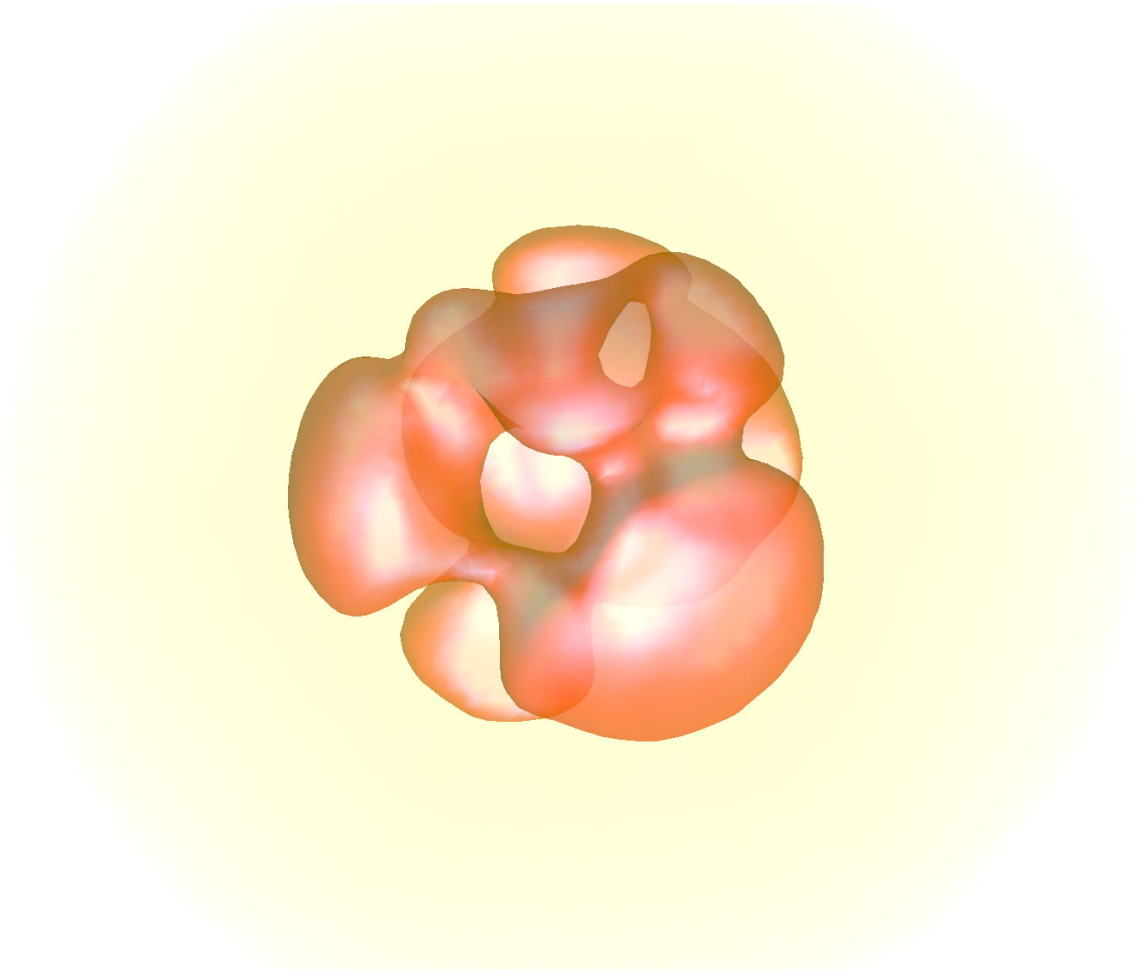

Figure 22. The expanding bubbles in 3D simulation following core collapse. From Los Alamos press release.

W. Baade and F. Zwicky, Proc, Nat. Acad. Sci., **20**, 259 (1934)

H. A. Bethe, Phys. Rev. **55**, 434 (1939)

H. A. Bethe and C. L. Critchfield, Phys. Rev. **54**, 862 (1938)

E. M. Burbidge, G. R. Burbidge, W. A. Fowler, and F. Hoyle, Revs. Modern Phys., **29**, 547 (1957)

A. G. W. Cameron, Astrophys. J., **121**, 144 (1955)

A. G. W. Cameron, Astrophys. J., **130**, 884 (1959)

A. G. W. Cameron, Astrophys. J., **562**, 456 (2001)

A. G. W. Cameron, Astrophys. J., in revision (2003)

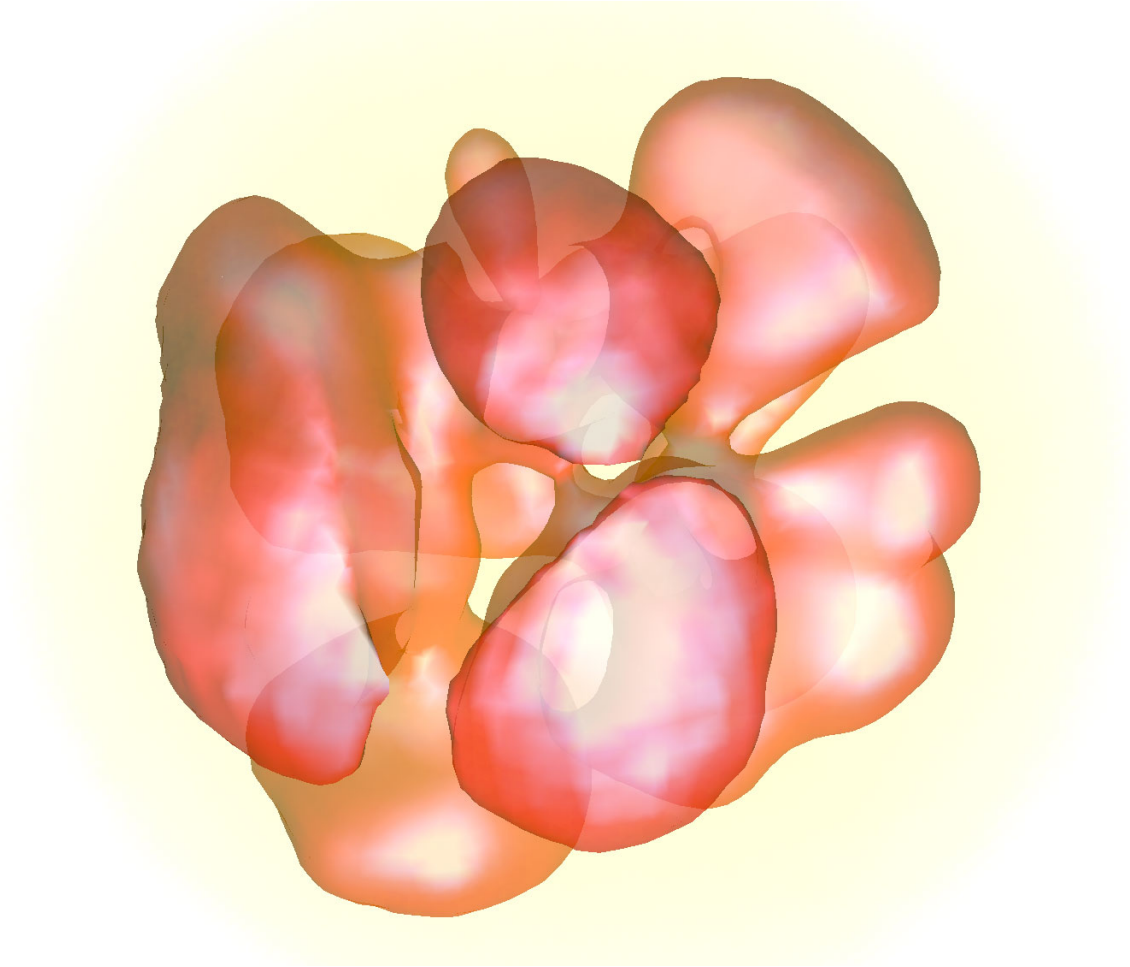

Figure 23. The expanding bubbles in 3D simulation a little later in the expansion. The asymmetries drive turbulent mixing in the outer layers of the supernova. From Los Alamos press release.

C. Freiburghaus, S. Rosswog, and F.-K. Thielemann, Astrophys. J., **525**, L121 (1999)

C. L. Fryer and M. S. Warren, Astrophys. J., **564**, L65 (2002)

G. Gamow, Zeits. f. Physik, **32**, 510 (1929)

R. W. Gurney and E. U. Condon, Phys. Rev. **33**, 127 (1929)

R. D. Hoffman, S. E. Woosley, and Y.-Z. Qian, Astrophys. J., **482**, 951 (1997)

F. Hoyle, Mon. Not. Roy. Astron. Soc., **106**, 343 (1946)

G. R. Huss and R. S. Lewis, Meteoritics, **29**, 971 (1994)

A. Königl and R. E. Pudritz, in *Protostars and Planets IV*, ed. V. Mannings, A. P. Boss, and S. S. Russell (Tucson, U. Arizona Press), 963 (2000)

M. Livio, Phys. Rep., **311**, 225 (1999)

P. W. Merrill, Astrophys. J., **116**, 21 (1952)

J. R. Oppenheimer and H. Snyder, Phys. Rev., **56**, 455 (1939)

J. R. Oppenheimer and G. M. Volkoff, Phys. Rev., **55**, 374 (1939)

Y.-Z. Qian and S. E. Woosley, Astrophys. J., **471**, 331 (1996)

M. Rayet, M. Arnould, M. Hashimoto, M. Prantzos, and K. Nomoto, Astron. Astrophys. **298**, 517 (1995)

J. H. Reynolds, Phys. Rev. Lett., **4**, 8 1960

E. E. Salpeter, Astrophys. J., **115**, 326 (1952)

R. Schneider, A. Ferrara, P. Natarajan, and K. Omukai, Astrophys. J., **571**, 30 (2002)

H. E. Suess and H. C. Urey, Revs. Modern Phys., **28**, 53 (1956)

H. A. T. Vanhala and A. P. Boss, Astrophys. J., **575**, 1144 (2002)

H. A. T. Vanhala and A. G. W. Cameron, Astrophys. J., **508**, 291 (1998)

G. J. Wasserburg, M. Busso, and R. Gallino, Astrophys. J., **466**, L109 (1996)

C. F. von Weizsäcker, Phys. Zs., **38**, 176 (1937)

C. F. von Weizsäcker, Phys. Zs., **39**, 633 (1938)